Supporting Information for

Fluorous soluble cyanine dyes for visualizing perfluorocarbons in living systems

Irene Lim[a], Antoine Vian[b], Heidi L. van de Wouw[a], Rachael A. Day[a], Carlos Gomez,[b] Yucen Liu,[b] Arnold L. Rheingold[c], Otger Campas[b,*], and Ellen M. Sletten[a,*]

[a]Department of Chemistry and Biochemistry, University of California, Los Angeles

[b]Department of Mechanical Engineering, University of California, Santa Barbara

[c]Department of Chemistry and Biochemistry, University of California, San Diego

*Corresponding email: campas@ucsb.edu, sletten@chem.ucla.edu

Table of Contents:

Supplemental figures

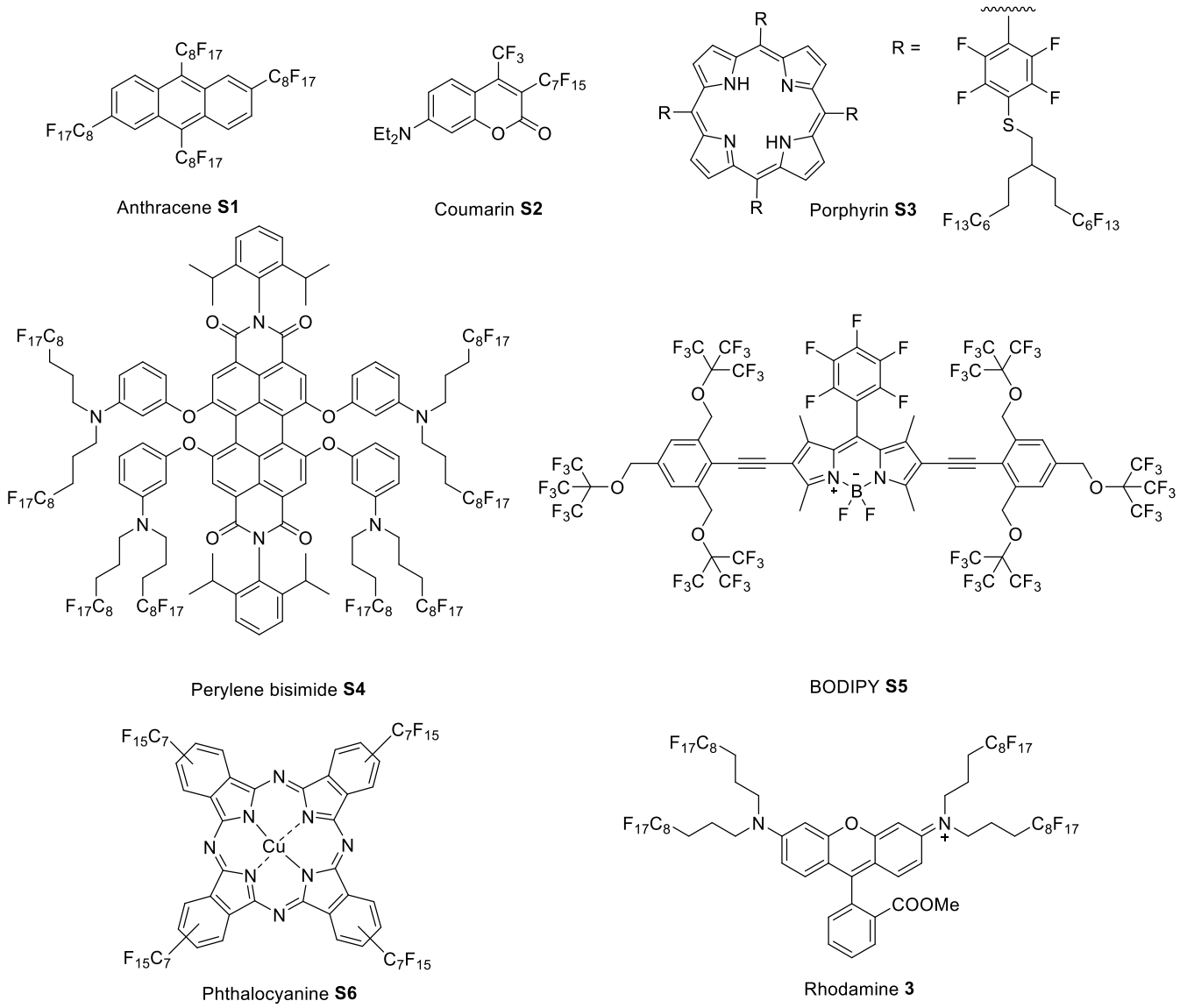

Figure S1: Structures of fluorofluorophores with greater than 50 wt% F listed in Figure 1.

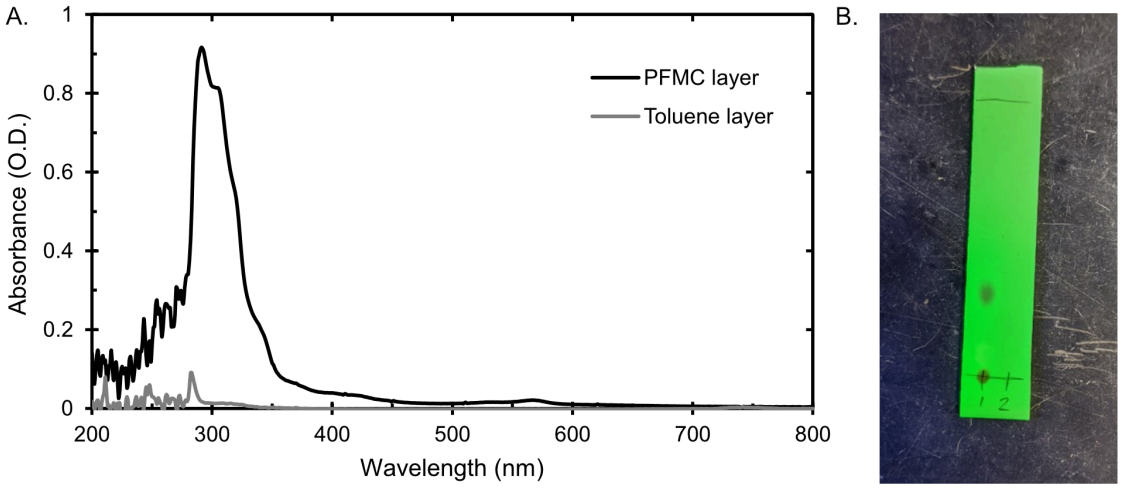

Figure S2: Solubility of indolenine **10** in fluorous solvent. After partitioning **10** between 2 mL of perfluoromethylcyclohexane and toluene (0.2 M), the layers were separated. A) A UV-Vis absorbance spectrum of **10** taken in PFMC and toluene. Both solvents absorb between 200 and 300 nm. B) A silica plate illuminated by shortwave UV light, spotted with PFMC layer (lane 1) and toluene layer (lane 2). The TLC plate was eluted in hexane (R_f = 0.35).

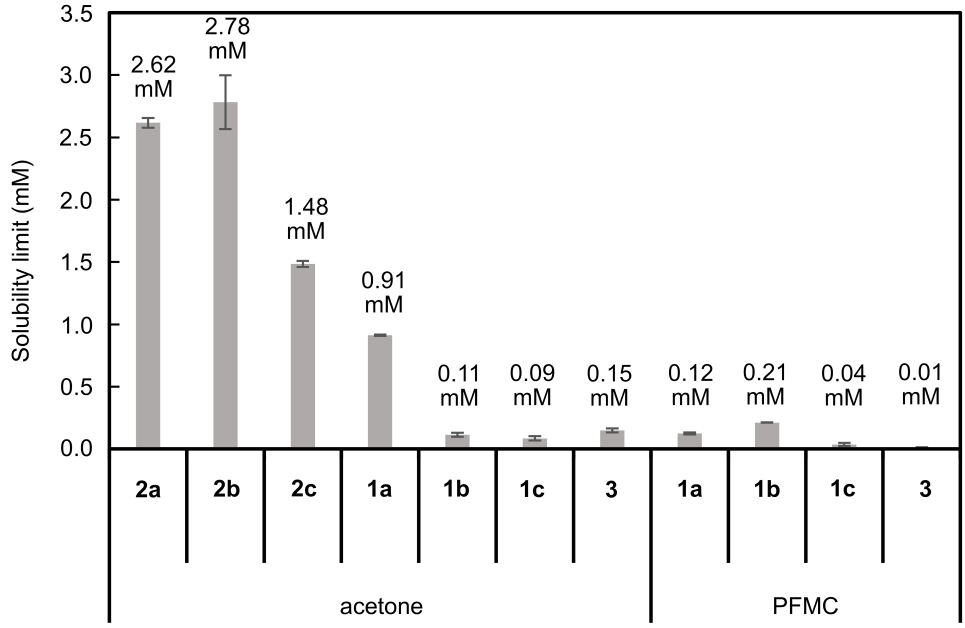

Figure S3: Absolute solubilities of dyes **1a–c**, **2a–c** and **3** in acetone or PFMC. Absolute solubilities were measured by forming saturated solutions. Saturated solutions were formed by adding excess dye to PFMC or acetone, then sonicating. After allowing the particulates to settle to the bottom of the vials, 10 µL of saturated solution was drawn up by Hamilton syringe from the top of the solution. These aliquots were evaporated to dryness, resuspended in acetone (200 µL) and the optical density was immediately measured. The optical density at λ_{max} was divided by the measured absorption coefficient of the dye in acetone (see Figure 3) to obtain concentration according to Beer's law where path length = 1 cm. Errors are standard deviations of two separate vials per condition. (See section below for more detail.)

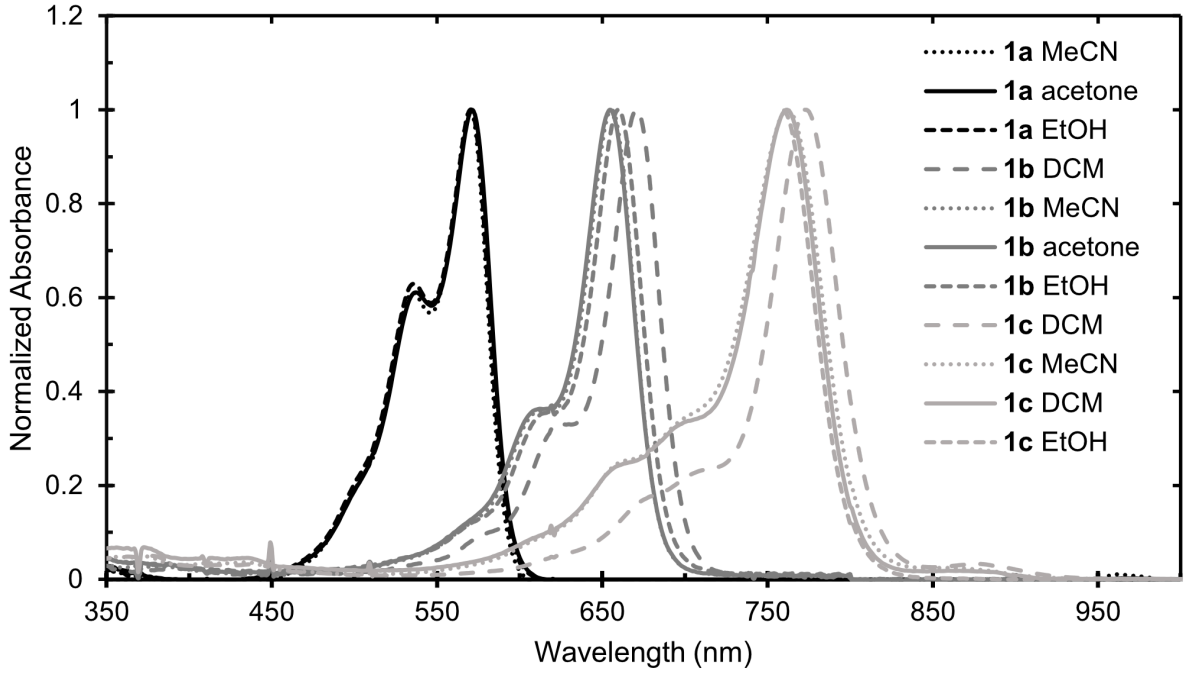

Figure S4: Absorbance spectra of cyanines **1a–1c** taken in organic solvents. All spectra are normalized to λ_{max}.

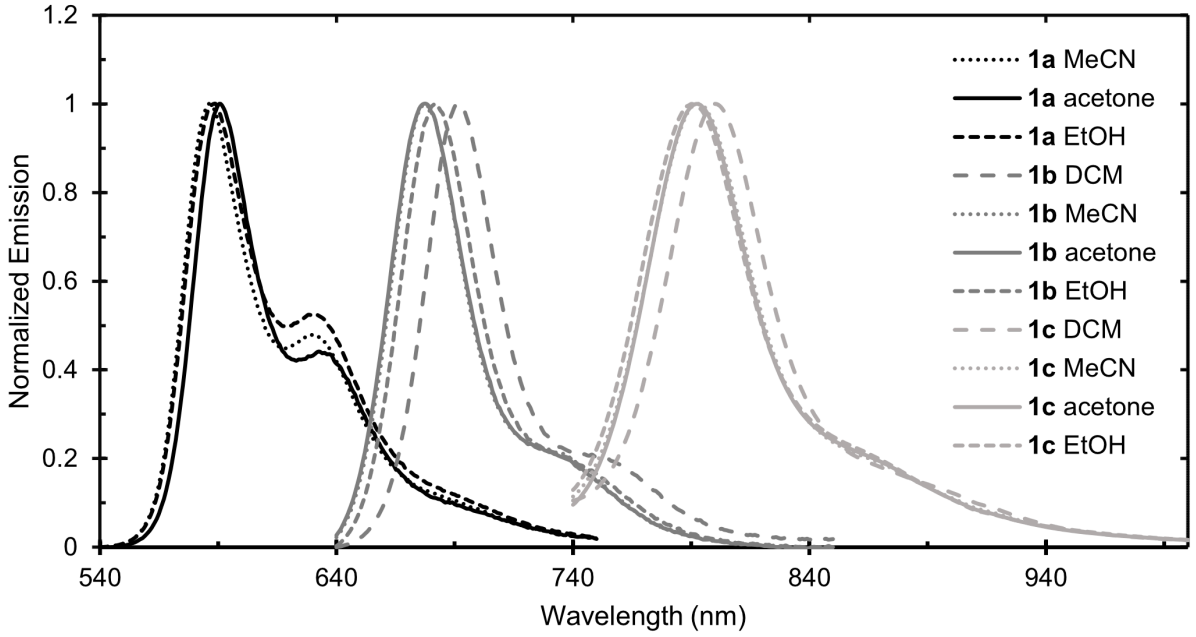

Figure S5: Emission spectra of cyanines **1a–1c** taken in organic solvents. All spectra are normalized to λ_{max}.

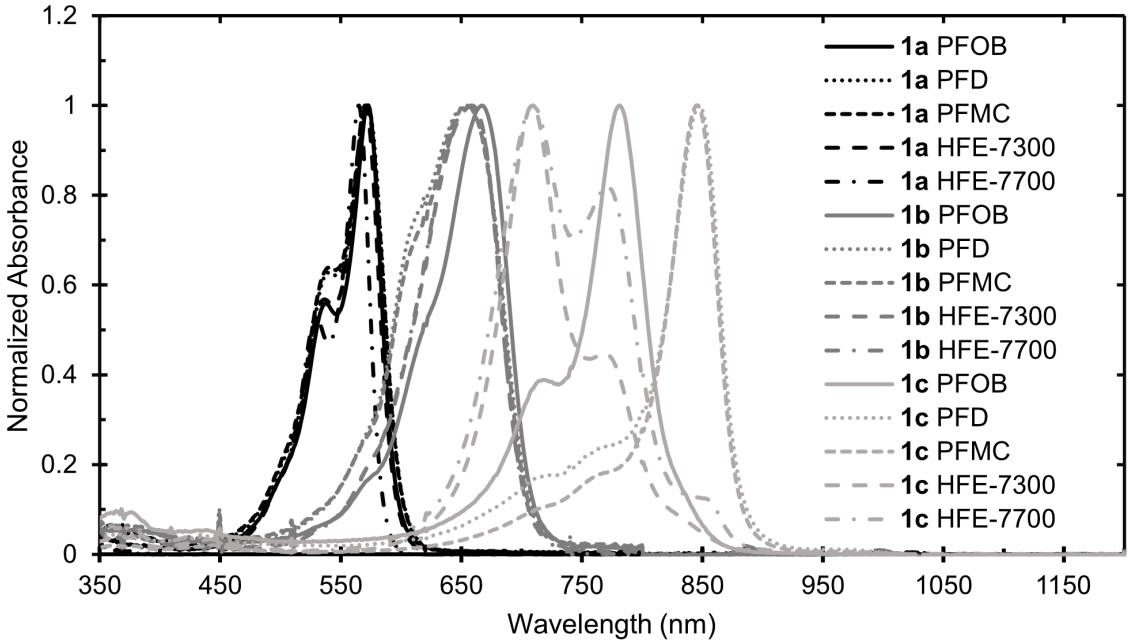

Figure S6: Absorbance spectra of cyanines **1a–1c** taken in fluorous solvents. All spectra are normalized to λ_{max}. See Figure S9 for fluorous solvent structures.

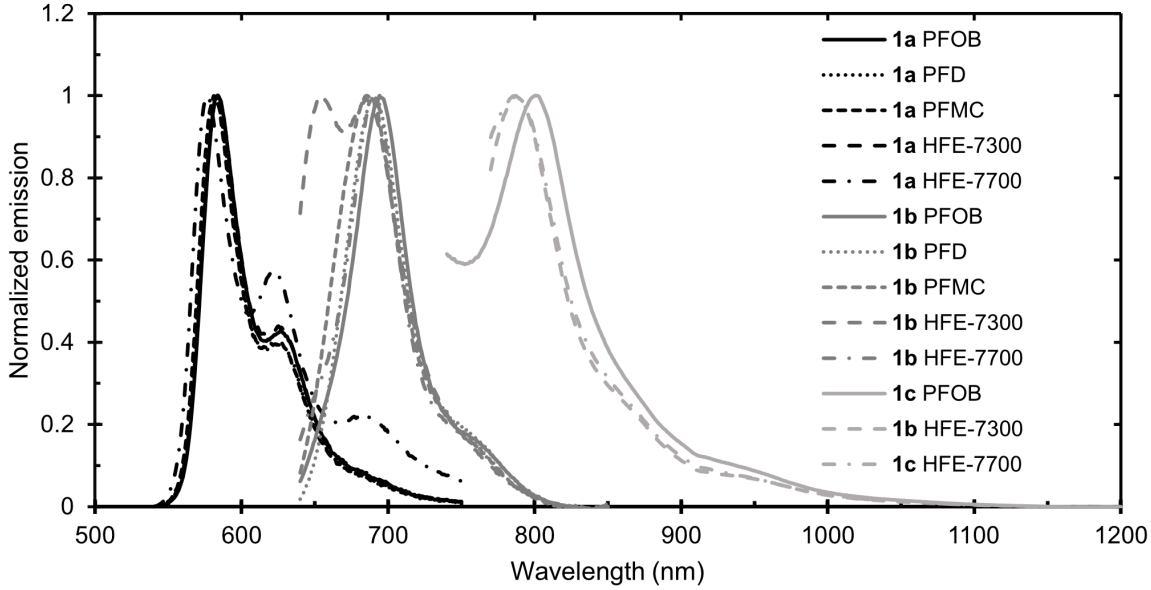

Figure S7: Emission spectra of dyes **1a–1c** taken in fluorous solvents. All spectra are normalized to λ_{max}. See Figure S9 for fluorous solvent structures.

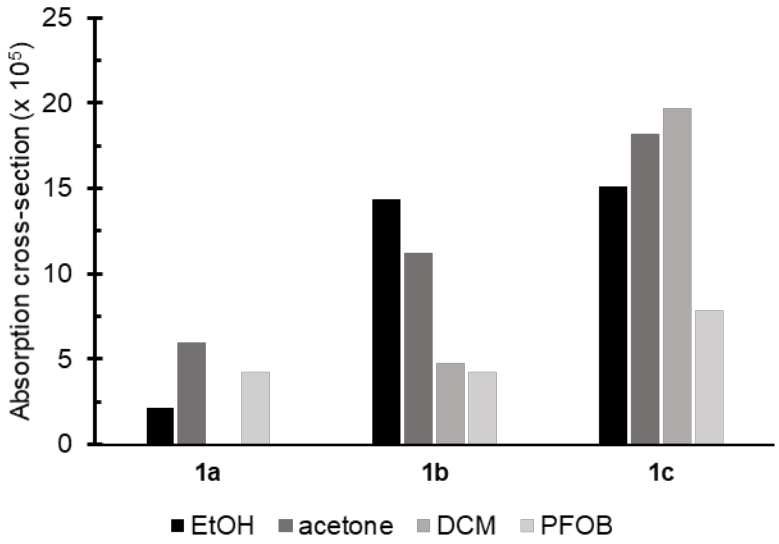

Figure S8: The area under the curve of absorption spectra for dyes **1a–1c**. Four solvents are represented.

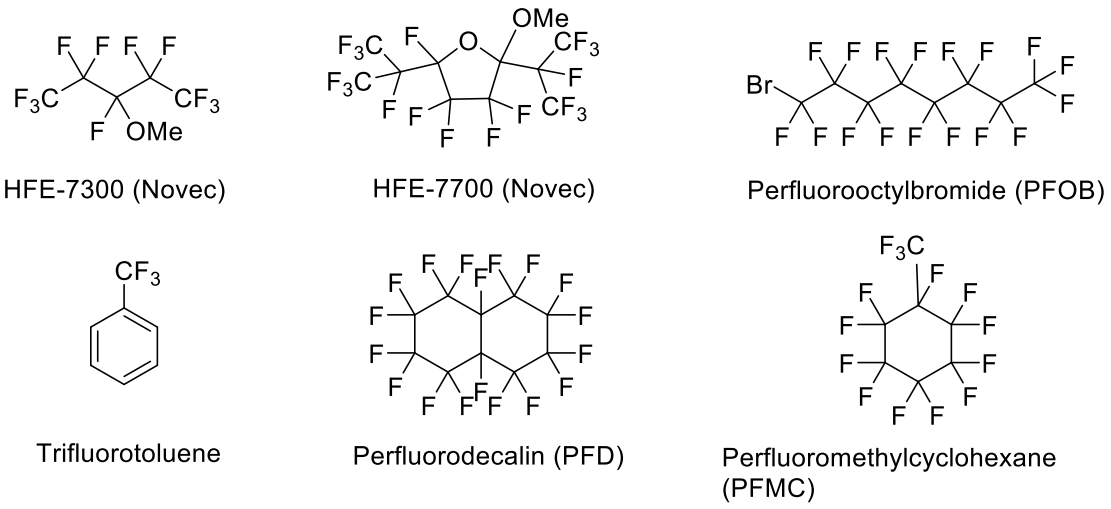

Figure S9: Structures and names of fluorous and semi-fluorinated solvents used in this manuscript.

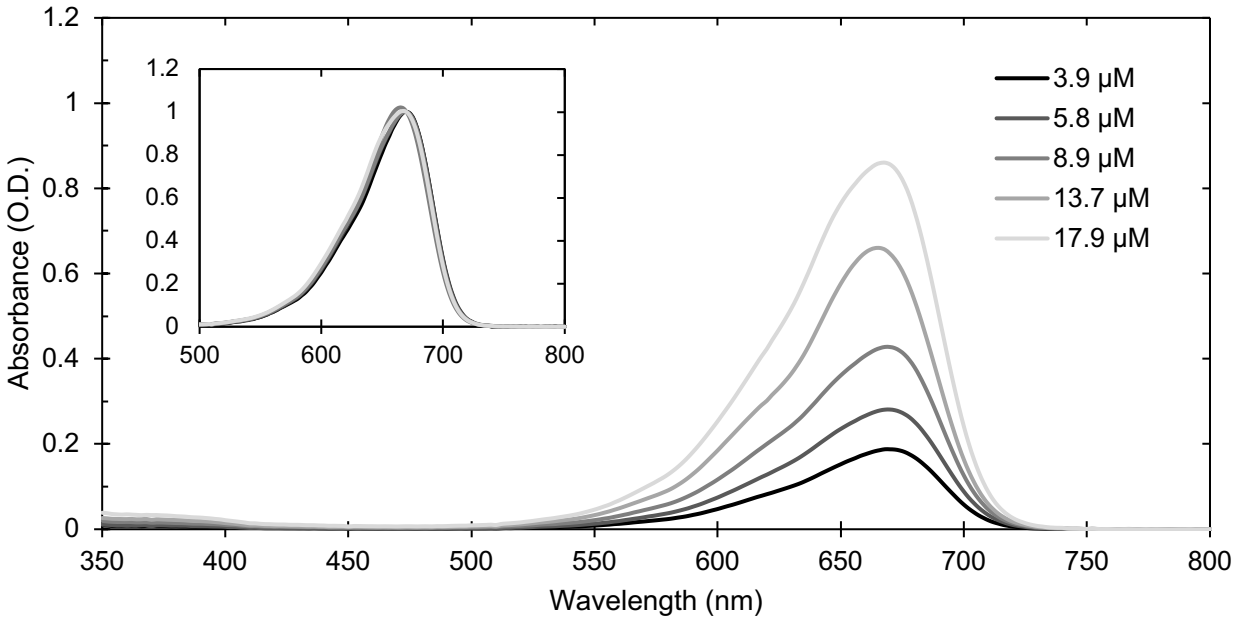

Figure S10: F_{86}Cy5 **1b** concentration study in PFOB. These data were obtained by serial dilution of F_{86}Cy5 in PFOB (3.9 µM, 5.8 µM, 8.9 µM, 13.7 µM, 17.9 µM). The inset shows all concentrations normalized indicating the spectra are not changed by concentration.

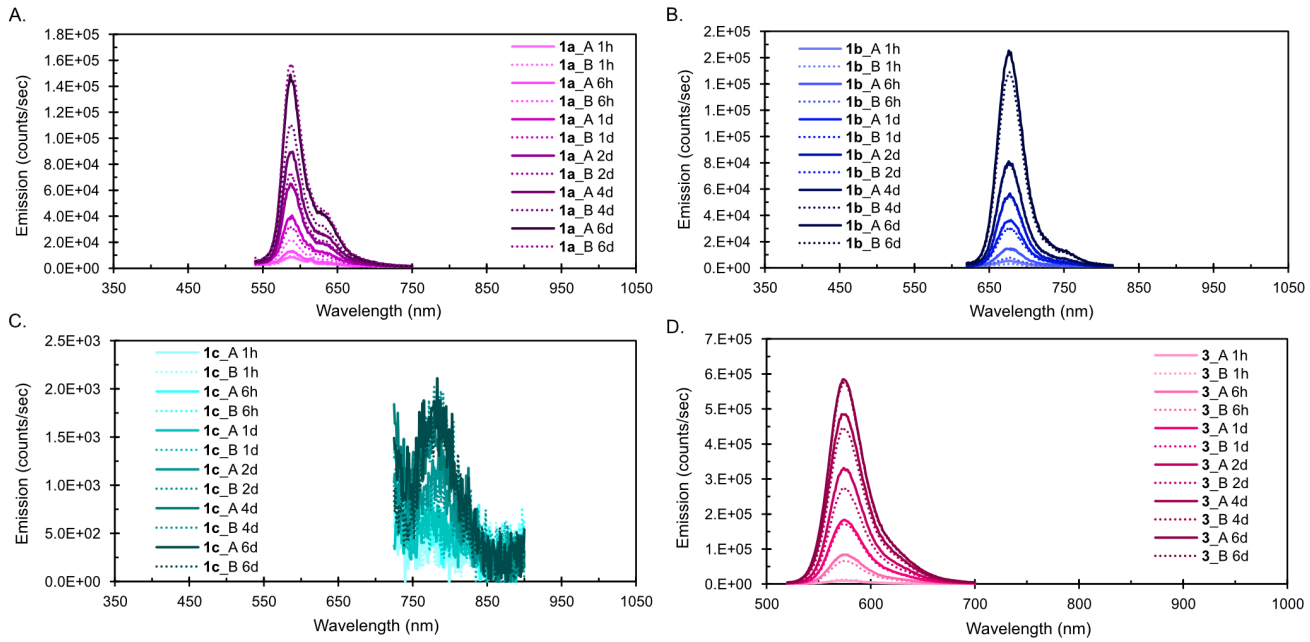

Figure S11: Emission spectra of dyes A) **1a**, B) **1b**, C) **1c**, and D) **3** in PFOB nanoemulsions stabilized by Pluronic F-68. Briefly, a 50 µL aliquot of dye-containing nanoemulsion solution was added to 950 µL of PBS in an Eppendorf tube. After pipetting several times, 500 µL 1-octanol was then layered on top of the nanoemulsion in PBS solution. The sealed Eppendorf tubes were rocked for a set amount of time (1 h, 6 h, 1 d, 2 d, 4 d, 6 d). At each time point, a 200 µL aliquot of the 1-octanol layer was removed from the tube, transferred to a quartz cuvette (3 mm), and the fluorescence spectrum was recorded. The 1-octanol solution was returned to the Eppendorf tube and allowed to continue to rock until further time points were collected.

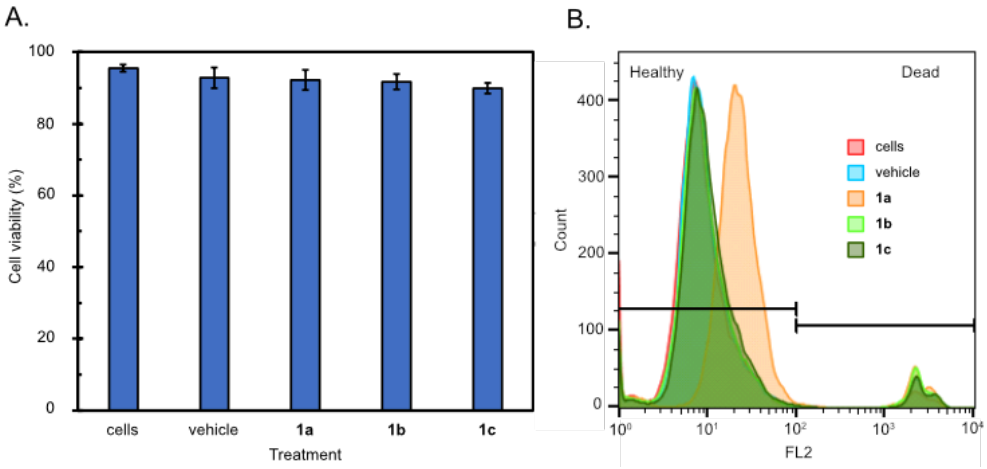

Figure S12: Cytotoxicity of emulsions containing fluorous cyanine dyes **1a–1c**. A) RAW cells were treated with nothing (cells), empty emulsions (vehicle), or **1a**-, **1b**- and **1c**-containing PFOB nanoemulsions (40 µL). After a 3 hour incubation period, cells were washed three times by centrifugation (526 x *g*, 3 min, 4 ˚C). Propidium iodide solution (2 µL in 1 mg/mL in PBS) was added to each well and the cells were transferred to FACS tubes with a final volume of 200 µL FACS buffer (PBS + 1% FBS). The cells were incubated on ice for 15 minutes prior to flow cytometry measurement. PI fluorescence was measured on FL2 channel. Data were analyzed by splitting the population at 10^2 as a live/dead line. Error bars represent the standard deviation of three replicates. $p > 0.05$ comparing vehicle to cells treated with **1a**–**1c**. B) Histograms corresponding to the data in A. Note that the live population that was treated with **1a** displays FL2 fluorescence due to emission from **1a**.

Supplemental Tables

Table S1: Top: Extinction coefficients and quantum yields measured in house, all values in EtOH. Bottom: Extinction coefficients and quantum yields measured in acetone.
Quantum yields were measured by petite integrating sphere in a Horiba fluorimeter. HICI (**2a**) and HIDCI (**2b**) were synthesized in house. HITCI (**2c**) was purchased from Sigma Aldrich.

EtOH	**$\lambda_{max,abs}$ (nm)**	**ε (x 10^5 $M^{-1}cm^{-1}$)**	**$\lambda_{max,em}$ (nm)**	**Φ_F**
2a	546	0.60 x 10^5 $\pm$ 0.01	563 nm	2.16% $\pm$ 0.07
2b	641	1.19 x 10^5 $\pm$ 0.02	664 nm	27.9% $\pm$ 0.3
2c	741	1.73 x 10^5 $\pm$ 0.02	768 nm	15.2% $\pm$ 0.8

acetone	**$\lambda_{max,abs}$ (nm)**	**ε (x 10^5 $M^{-1}cm^{-1}$)**	**$\lambda_{max,em}$ (nm)**	**Φ_F**
2a	545	0.53 $\pm$ 0.01	563	1.60% $\pm$ 0.01
2b	639	1.20 $\pm$ 0.02	663	11% $\pm$ 1
2c	741	1.61 $\pm$ 0.06	766	12.4% $\pm$ 0.7

Table S2: Corrected photobleaching rate constants. See section below for photobleaching calculations.

Solvent	**Dye**	**log(k_{rel})**
EtOH	**1a**	0
	1c	13.706
	2c	13.589
	3	15.8
PFOB	**1a**	14.76
	1b	13.26
	1c	12.4773
	3	15.10
O_2-free PFOB	**1a**	15.589
	1c	14.1816

Table S3: Nanoemulsion size analysis: An aliquot of freshly prepared emulsion solution (20 μL) was diluted in MilliQ H_2O (2 mL) in a plastic 1 cm cuvette.

Dye in NE	Z-Average Diameter[a] (nm)	Polydispersity [a]
1a	231 ± 4	0.08 ± 0.01
1b	251 ± 5	0.14 ± 0.03
1c	189 ± 1	0.07 ± 0.03
3	245 ± 5	0.12 ± 0.01

[a] Size was analyzed with a Malvern Zetasizer Nano dynamic light scattering instrument (10 runs, 10 seconds/run, three measurements, no delay between measurements, 25 °C with 120 second equilibration time). Data are representative of three replicate measurements.

Synthetic chemistry procedures (Figure 2)

Abbreviations

DCM: dichloromethane, methylene chloride; DMF: dimethyl formamide; DMSO: dimethyl sulfoxide; EtOAc: ethyl acetate; EtOH: ethanol; HCl: hydrochloric acid; hex: hexane; HFIP: hexafluoroisopropanol; K_2CO_3: potassium carbonate; MeCN: acetonitrile; $MgSO_4$: magnesium sulfate; SiO_2: silica gel; THF: tetrahydrofuran.

Materials

Ethyl cyanoacetate, 2,6-di-*tert*-butyl-4-methylpyridine, iodoform, and 2,6-lutidine were purchased from Sigma-Aldrich. Acetic anhydride and triethyl amine were purchased from EMD. 1-Iodo-1*H*,1*H*,2*H*,2*H*-perfluorooctane was purchased from Synquest Laboratories. Potassium carbonate was purchased from Amresco. DMSO was purchased from BDH. 1 M Methyl magnesium bromide in THF and acetic acid were purchased from Acros Organics. Phenylhydrazine hydrochloride was purchased from TCI America.

Anhydrous solvents were dispensed directly from a Grubb's-type Phoenix Solvent Drying System constructed by JC Meyer or kept dry under sieves in a Schlenk bomb. All chemicals were used as received unless otherwise stated. All reactions were done under dry Schlenk technique unless otherwise noted.

Instrumentation

Microwave reactions were performed using a CEM Discover SP microwave synthesis reactor. All reactions were performed in glass 10 mL microwave reactor vials purchased from CEM with silicone/PTFE caps. Flea micro PTFE-coated stir bars were used in the vials with magnetic stirring set to high and 15 seconds of premixing prior to the temperature ramping. All microwave reactions were carried out with the pressure release limit set to 250 psi (no reactions exceeded this limit to trigger venting) and the maximum wattage set to 300 W (the power applied was dynamically controlled by the microwave instrument and did not exceed this limit for any reactions). Thin layer chromatography was performed with Silica Gel 60 F254 (EMD Millipore) plates and visualized with UV light. Flash chromatography was executed with technical grade silica gel purchased from Sorbtech Technologies with 60 Å pores and 40 – 63 μm mesh particle size. Flash column chromatography was performed on technical grade silica gel with 60 Å pores and 40–63 μm mesh particle size (Sorbtech Technologies). Solvent was removed by rotary evaporation on a Büchi Rotovapor with a Welch self-cleaning dry vacuum pump and further dried by reduced pressure with a Welch DuoSeal pump. Melting points were measured with DigiMelt MPA160 melting point apparatus.

All ^{1}H NMR, ^{13}C{^{1}H} NMR, and ^{19}F{^{1}H} NMR spectra were recorded on a Bruker AV-400 (^{1}H, ^{19}F{^{1}H}), Bruker Avance-500 (^{1}H, ^{13}C{^{1}H}), or AV-300 (^{1}H, ^{19}F{^{1}H}) instruments at the UCLA Molecular Instrumentation Center and chemical shifts are reported in parts per million (ppm). Spectra were recorded in chloroform ($CDCl_3$), acetone-d_6, or hexafluoroisopropanol (HFIP-d_2) and referenced to residual solvent peak. Multiplicities are as indicated: s (singlet), d (doublet), t (triplet), q (quartet), qn (quintet), m (multiplet), bs (broad singlet), and bm (broad multiplet). Coupling constants, *J*, are reported in Hertz (Hz) and integration is provided, along with assignments, as indicated. Mass spectrometry were performed by matrix assisted laser desorption ionization (MALDI) time of flight (TOF) analysis on a Bruker Ultraflex MALDI TOF-TOF or by electrospray ionization (ESI) on a Waters LCT Premier TOF LC/MS with ACQUITY UPLC. Masses for analytical measurements were taken on a Sartorius MSE6.6S-000-DM

Cubis Micro Balance. Bath sonication was performed using a Branson 3800 ultrasonic cleaner. Probe sonication for nanoemulsion preparation was performed using a QSonica (Q125) probe sonicator. Dynamic light scattering measurements were performed on a Malvern Zetasizer Nano dynamic light scattering instrument. SOP parameters: 10 runs, 10 seconds/run, three measurements, no delay between measurements, 25 °C with 120 second equilibration time. Data are representative of three replicate measurements.

Synthetic procedures

Synthesis of 2,2-bis((perfluorohexyl)ethyl) ethyl cyanoacetate, **S7**:

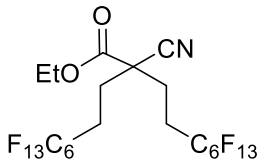

To a dry 2-neck flask under positive N_2 pressure, 1,1,1,2,2,3,3,4,4,5,5,6,6-tridecafluoro-8-iodooctane (4.50 mL, 18.2 mmol, 2.06 eq) and ethyl cyanoacetate (940 µL, 8.83 mmol, 1.00 equiv) were added. As this mixture is biphasic, it is stirred vigorously (>600 rpm). To the flask is added DMF (12.0 mL, anhydrous) and K_2CO_3 (2.68 g, 19.4 mmol, 2.20 equiv). Over three days, this mixture is stirred at 50 °C in an oil bath. Alternatively, periodic heat gun application also keeps this reaction mixture homogeneous. After 72 hours, the product is crashed out by addition of water (200 mL) and filtered to yield off-white solid **S7** in 92% yield (8.12 mmol). ^{1}H-NMR (300 MHz, $CDCl_3$): δ 4.36 (q, J = 4.2 Hz, 2 H), 2.30 (m, 4 H), 2.16 (m, 4 H), 1.36 (t, J = 7.1 Hz, 2H). ^{1}H-NMR matches literature.[1]

Synthesis of 2,2-bis((perfluorohexyl)ethyl)ethylnitrile, **7**:

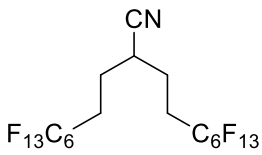

To a dry 2-neck flask with reflux condenser attached, **S7** (3.00 g, 3.73 mmol, 1.00 equiv), lithium chloride (520 mg, 12.3 mmol, 3.30 equiv), DMSO (28.6 mL) and milliQ water (945 µL) was added. The reaction was refluxed at 160 °C overnight (14-16 h). After cooling, the reaction was extracted in ether and water (5 x 30 mL) and the organic layer collectively dried with $MgSO_4$. The off-white solid was used without further purification (2.50 g, 83% yield). ^{1}H-NMR (300 MHz, $CDCl_3$): δ 2.82-2.75 (quintet, J = 6.0, 3 Hz, 1H), 2.27-2.21 (m, 4H), 2.03-1.96 (m, 4H). ^{1}H-NMR matches literature.[1]

Synthesis of 6,6,7,7,8,8,9,9,10,10,11,11,11-tridecafluoro-3-(3,3,4,4,5,5,6,6,7,7,8,8,8-tridecafluorooctyl)-undecan-2-one, **8**:

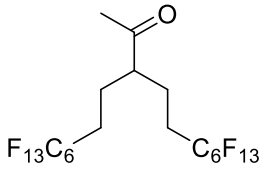

To a flame dried reaction flask, **7** (2.50 g, 3.41 mmol, 1.00 equiv) in dry THF (57.0 mL) was added, followed by dropwise addition of methyl Grignard (1 M, 17.06 mmol, 5.000 equiv). The reaction was refluxed at 65 °C for 5 hours. After cooling, the reaction was quenched with distilled water (~ 3 mL) followed by 1 M HCl (2 mL). After extraction in ethyl acetate (3 x 30 mL), the organic layer was dried over $MgSO_4$ and adsorbed onto SiO_2. The product was purified by column chromatography, eluting with 20:1 hexane:EtOAc. A yellow sticky oil was obtained in 59% yield (1.510 g, 2.013 mmol). ^{1}H-NMR (300 MHz, $CDCl_3$) δ 2.67 (quintet, J = 6.0 Hz, 1H), 2.20 (s, 3H), 2.13 – 1.91 (m, 5H), 1.84 – 1.63 (m, 2H). ^{19}F NMR (282 MHz, $CDCl_3$) δ -81.2 (t, J = 20.33, 6F) , -114.7 (bs, 4F), -122.1 (bs, 4F), -123.1 (bs, 4F), -123.6 (bs, 4F), -126.4 (bs, 4F). ^{13}C-NMR (126 MHz, $CDCl_3$): δ 209.2, 118.3-113.7 (m, CF_n peaks), 50.1, 29.0, 28.1 (t, J_{CF} = 22.3 Hz), 21.3 (t, J = 3.9 Hz). HRMS (ESI+): Calculated for $C_{14}H_{12}F_{15}O^+$ $[M–C_5F_{11}]^+$: 481.0649; found: 481.0644.

Synthesis of 2-methyl-3,3-bis(3,3,4,4,5,5,6,6,7,7,8,8,8-tridecafluorooctyl)-3H-indole, **9**:

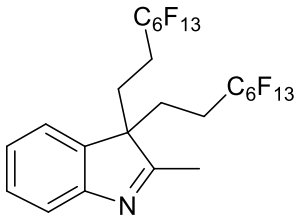

To a scintillation vial charged with stir bar, ketone **8** (1.29 g, 1.72 mmol, 1.00 equiv) was added. The reaction vessel was dried *in vacuo*; then phenylhydrazine hydrochloride (249 mg, 1.72 mmol, 1.00 equiv) and acetic acid (0.40 M, 4.30 mL) were added. Addition of reflux cap allowed for heating to 120 °C and the reaction was stirred for 24 hours. After cooling, the mixture was extracted in DCM and washed with distilled water (3 x 10 mL). After drying with $MgSO_4$, the organic layer was adsorbed onto silica. The crude mixture was chromatographed in 4:1 hexane:toluene, then 1:1 hexane:toluene, and toluene. The product eluted in toluene (R_f = 0.48 in 4:1 hexane:EtOAc) as a mustard yellow solid obtained in 43% yield (605 mg, 0.734 mmol). ^{1}H NMR (500 MHz, $CDCl_3$) δ 7.59 (d, *J* = 7.7 Hz, 1H), 7.47 – 7.36 (m, 1H), 7.31 (d, *J* = 7.9 Hz, 1H), 7.24 (d, *J* = 7.3 Hz, 1H), 2.24 – 2.08 (m, 4H), 1.43 – 1.27 (m, 3H). ^{19}F NMR (282 MHz, $CDCl_3$) δ -80.9 (s, 6F), -114.1 (m, 4F), -122.1 (bs, 4F), -123.1 (bs, 8F), -126.2 (bs, 4F). ^{13}C NMR (126 MHz, $CDCl_3$) δ 182.7, 154.9, 138.1, 129.2, 126.5, 121.3, 120.8, 60.0, 29.7, 26.8, 25.7, 15.4. HRMS (ESI^+): Calculated for $C_{25}H_{16}F_{26}N^+$ $[M+H]^+$: 824.0862; found: 824.0841.

Synthesis of 1-(4,4,5,5,6,6,7,7,8,8,9,9,10,10,11,11,11-heptadecafluoroundecyl)-2-methylene-3,3-bis(3,3,4,4,5,5,6,6,7,7,8,8,8-tridecafluorooctyl)indoline, **10**:

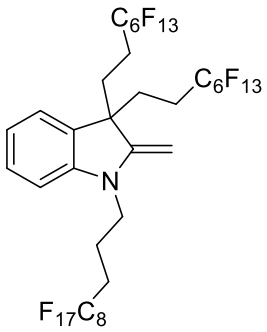

To a microwave vial, indole **9** (775 mg, 0.941 mmol, 1.00 equiv), 1,1,1,2,2,3,3,4,4,5,5,6,6,7,7,8,8-heptadecafluoro-11-iodoundecane **S8** (1.235 g, 2.100 mmol, 2.230 equiv), 2,6-lutidine (220 µL, 1.88 mmol, 2.00 equiv), and acetonitrile (6.7 mL, 0.14 M) were added. The reaction was placed in the microwave (150 W, 160 °C, 8 hr). The crude dark red biphasic mixture was directly adsorbed onto silica and purified by flash chromatography. Excess perfluoroalkyl iodide **S8** was eluted from the column first with no air pressure. The desired product was then collected in hexane with air pressure (890 mg, 0.693 mmol, 74% yield). The product, a colorless oil, was only moderately stable and should be stored under N_2 in the freezer. F_{86}Cy3 **1a** can also be collected from this reaction in 3% yield by eluting 10% ethanol and DCM, after all other by-products have eluted. R_f of **10** = 0.28 in hexane. ^{1}H-NMR (500 MHz, $CDCl_3$): δ 7.23 (td, *J* = 7.7, 1.1 Hz, 1H), 7.07 (dd, *J* = 7.4, 0.9 Hz, 1H), 6.89 (td, *J* = 7.5, 0.5 Hz, 1H), 6.657 (d, *J* = 7.9 Hz, 1H), 4.05 (bd, *J* = 72.9 Hz, 2H), 3.64 (t, *J* = 6.8 Hz, 2H), 2.15–2.09 (bm, 4H), 1.99–1.83 (bm, 6H), 1.46–1.32 (bm, 2H). ^{19}F-NMR (376 MHz, $CDCl_3$): δ -80.9 (t, *J* = 9.9 Hz, 3F), -81.0 (t, *J* = 9.9 Hz, 6F), -113.9 (quintet, *J* = 15.8 Hz, 4F), -114.5 (t, *J* = 15.1 Hz, 2F), -122.1 (bs, 10F), -123.1 (bs, 6F), -123.4 (bs, 6F), -126.3 (bm, 6F). ^{13}C-NMR (126 MHz, $CDCl_3$): δ 146.9, 129.4 (d, *J* = 16.8 Hz), 122.5, 120.5-108.7 (m, CF_n peaks) 120.3, 105.6, 50.8, 41.5, 33.0, 29.9, 28.8 (t, *J* = 23.0 Hz), 26.7 (t, *J* = 22.1 Hz), 17.9. HRMS (ESI^+): Calculated for $C_{36}H_{21}F_{43}N^+$ $[M]^+$: 1284.0982; found: 1284.0929.

Synthesis of 1-(4,4,5,5,6,6,7,7,8,8,9,9,10,10,11,11,11-heptadecafluoroundecyl)-2-((E)-3-((E)-1-(4,4,5,5,6,6,7,7,8,8,9,9,10,10,11,11,11-heptadecafluoroundecyl)-3,3-bis(3,3,4,4,5,5,6,6,7,7,8,8,8-tridecafluorooctyl)indolin-2-ylidene)prop-1-en-1-yl)-3,3-bis(3,3,4,4,5,5,6,6,7,7,8,8,8-tridecafluorooctyl)-3H-indol-1-ium chloride, **1a**:

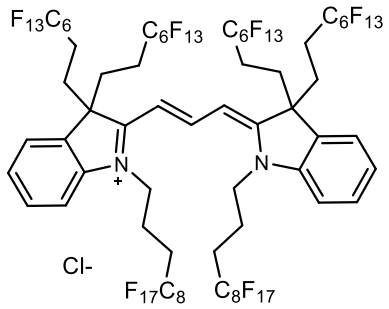

In a glass LCMS vial charged with stir bar, fluorous indoline **10** (25.3 mg, 0.0139 mmol, 2.00 equiv), iodoform (2.7 mg, 0.0069 mmol, 1.0 equiv) and 2,6-di-*tert*-butyl-4-methylpyridine (5.8 mg, 0.028 mmol, 4.1 equiv) were dissolved in acetic anhydride (100 µL, 0.14 M). The mixture was heated to 140 °C for 2.5 hours. The crude product was dissolved in acetone and adsorbed onto silica and purified by flash chromatography using a DCM:EtOH solvent system (DCM → 1:100 → 2:100 → 3:100 → 4:100 → 5:100 → 10:100 ethanol:DCM). Indoline **10** eluted with 2:100 EtOH:DCM. The overall yield of the dark pink solid is 0.7% (0.0000483 mmol, 0.127 mg). $\lambda_{max,abs}$ (acetone) = 571 nm. $\lambda_{max,em}$ (acetone) = 591 nm. ^{1}H-NMR (500 MHz, HFIP-d_2): δ 8.64 (t, *J* = 13.3 Hz, 1H), 7.66 (t, *J* = 7.5 Hz, 2H), 7.57 (t, *J* = 7.5 Hz, 2H), 7.52 (d, *J* = 7.5 Hz, 2H), 7.32 (d, *J* = 8.2 Hz, 2H), 6.42 (d, *J* = 11.0 Hz, 2H), 4.28 (t, *J* = 6.4 Hz, 4H), 2.80 (t, *J* = 10.4 Hz, 4H), 2.61 (t, *J* = 11.4 Hz, 4H), 2.34 (bm, 4H), 2.23 (t, J = 6.3 Hz, 4H), 1.71 (bm, 5H), 1.54 (bm, 5H). ^{19}F-NMR (376 MHz, $CDCl_3$): δ -81.8 (tt, *J* = 72.4, 9.9 Hz, 18F), -114.6 (tq, *J* = 313.6, 15.4 Hz, 10F), -122.5 (m, *J* = 44.5 Hz, 23F), -123.8 (m, *J* = 88, 84 Hz, 24F), -126.7 (m, 12F). Melting point: 63.3–65.5 °C. MALDI-TOF MS (ESI$^+$): Calculated for $C_{73}H_{39}F_{86}N_2^+$ [M]$^+$: 2577.1735; found: 2579.0807.

Synthesis of 1-(4,4,5,5,6,6,7,7,8,8,9,9,10,10,11,11,11-heptadecafluoroundecyl)-2-((1E,3E)-5-((E)-1-(4,4,5,5,6,6,7,7,8,8,9,9,10,10,11,11,11-heptadecafluoroundecyl)-3,3-bis(3,3,4,4,5,5,6,6,7,7,8,8,8-tridecafluorooctyl)indolin-2-ylidene)penta-1,3-dien-1-yl)-3,3-bis(3,3,4,4,5,5,6,6,7,7,8,8,8-tridecafluorooctyl)-3H-indol-1-ium chloride, **1b**:

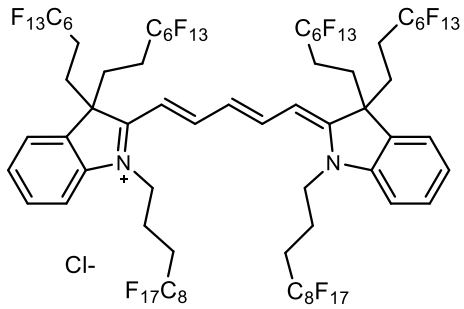

In a glass LCMS vial charged with stir bar, fluorous indoline **10** (65.2 mg, 0.0357 mmol, 2.00 equiv), malonaldehyde bis(phenylimine) **6b** (4.6 mg, 0.018 mmol, 1.0 equiv), and 2,6-lutidine (8.2 µL, 0.072 mmol, 4.0 equiv), and acetic anhydride (0.25 M, 140 µL) were added. The reaction mixture was freeze-pump-thawed (x3) and heated to 140 °C while monitoring by UV-Vis for reaction completion, at which point it was cooled to room temperature and washed in brine. The crude product was adsorbed onto silica and purified via flash chromatography using DCM:ethanol as the eluent (DCM → 1:100 → 2:100 → 3:100 → 4:100 → 5:100 → 10:100 ethanol:DCM). The product eluted with 2:100 ethanol:DCM. The fractions deemed pure by UV-Vis were collected and dried *in vacuo* and crystallized from acetone. The crystals were collected as pure **1b** (4.4 mg, 0.0017 mmol, 9% yield). $\lambda_{max,abs}$ (DCM) = 672 nm. $\lambda_{max,em}$ (DCM) = 691 nm. ^{1}H-NMR (500 MHz, acetone-d_6): δ 7.77 (d, *J* = 7.4 Hz, 1H), 7.66 (d, *J* = 8.1 Hz, 2H), 7.63 (d, *J* = 8.1 Hz, 1H), 7.56 (t, *J* = 7.5 Hz, 1H), 7.40 (t, *J* = 7.3 Hz, 1H), 7.25 (t, *J* = 7.8 Hz, 2H), 7.10 (d, *J* = 12.7 Hz, 1H), 7.00 (t, *J* = 7.3 Hz, 1H), 4.59 (t, *J* = 7.1 Hz, 1H), 1.90 (m, 3H), 1.50 (m, 5H). ^{19}F-NMR (376 MHz, acetone-d6): δ -81.7 (t, *J* = 9.9 Hz, 13F), -82.0 (t, *J* = 9.2 Hz, 5F), -114.6 (t, *J* = 16.1 Hz, 11F), -

122.4 (bs, 14F), -123.4 (bs, 10F), -123.7 (bs, 14F), -126.8 (m, 12F). Melting point: 58.7–60.6 °C. MALDI-TOF MS (ESI$^+$): Calculated for $C_{75}H_{41}F_{86}N_2^+$ [M]$^+$: 2603.1891; found: 2603.6034.

Synthesis of 1-(4,4,5,5,6,6,7,7,8,8,9,9,10,10,11,11,11-heptadecafluoroundecyl)-2-((1E,3E,5E)-7-((E)-1-(4,4,5,5,6,6,7,7,8,8,9,9,10,10,11,11,11-heptadecafluoroundecyl)-3,3-bis(3,3,4,4,5,5,6,6,7,7,8,8,8-tridecafluorooctyl)indolin-2-ylidene)hepta-1,3,5-trien-1-yl)-3,3-bis(3,3,4,4,5,5,6,6,7,7,8,8,8-tridecafluorooctyl)-3H-indol-1-ium chloride, **1c**:

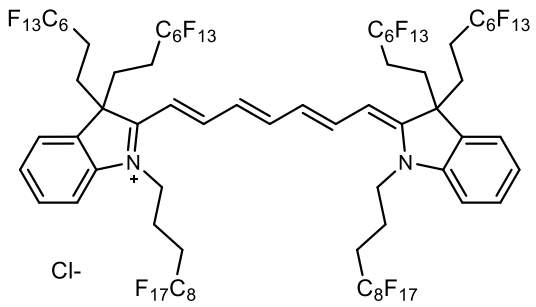

To a glass LCMS vial, fluorous indoline **10** (54 mg, 0.030 mmol, 2.0 equiv), glutaconaldehydedianil **6c** (4.2 mg, 0.015 mmol, 1.0 equiv), 2,6-di-*tert*-butyl-4-methylpyridine (19 mg, 0.094 mmol, 6.3 equiv), and acetic anhydride (0.25 M, 119 µL) were added. The reaction mixture was freeze-pump-thawed (x3) and heated to 140 °C while monitoring by UV-Vis for reaction completion, at which point it was cooled to room temperature and washed in brine. The crude product was adsorbed onto silica and purified by flash chromatography with a DCM:ethanol eluent (DCM → 1:100 → 2:100 → 3:100 → 4:100 → 5:100 → 10:100 ethanol:DCM). The product was eluted at 1:100 ethanol:DCM. The fractions deemed pure by UV-Vis were collected and dried *in vacuo*. The dark green solid was washed with cyclohexane (3 x 10 mL) and ethanol (3 x 20 mL) to yield 9.6 mg of **1c** (0.0035 mmol, 24% yield.) $\lambda_{max,abs}$ (DCM) = 773 nm. $\lambda_{max,em}$ (DCM) = 800 nm. ^{1}H-NMR (500 MHz, HFIP-d_2): δ 7.93 (t, J = 12.9 Hz, 1H), 7.59 (quintet, J = 4.15 Hz, 1H), 7.46 (d, J = 4.15 Hz, 1H), 7.20 (d, J = 8.1 Hz, 1H), 6.70 (t, J = 12.5 Hz, 1H), 6.32 (d, J = 13.4 Hz, 1H), 4.16 (t, J = 6.6 Hz, 2H), 2.64 (quintet, J = 14.6 Hz, 4H), 2.34 (m, J = 7.4 Hz, 2H), 2.19 (quintet, J = 7.0 Hz, 2H), 1.75 (quintet, J = 14.4 Hz, 2H), 1.48 (bm, 3H). ^{19}F-NMR (376 MHz, $CDCl_3$): δ -80.9 (m, J = 10.3, 8.5 Hz, 18F), -113.8 (d, J = 112 Hz, 11F), -122.2 (bs, 17F), -122.6 (s, 3F), -123.0 (bs, 21F), -126.3 (bs, 12F). Melting point: 91.4–93.8 °C. MALDI-TOF MS (ESI$^+$): Calculated for $C_{77}H_{43}F_{86}N_2^+$ [M]$^+$: 2629.2048; found: 2628.9345.

Fluorous solubility (Figure 3B-C)

Fluorous partition (PFMC/toluene). From stock solutions of dyes in ethanol, a few drops were added to vials and ethanol was evaporated. To the vials, toluene (3 mL) and perfluoromethylcyclohexane (PFMC, 3 mL) were added. All vials were capped, and shaken vigorously by hand (10 seconds) and vortexed (10 seconds). The layers were allowed to separate and aliquots from each layer (200 μL) were portioned into test tubes. As PFMC has a low boiling point and toluene does not, the PFMC was evaporated, then toluene (200 μL) was added to keep the solvent composition of all samples the same. At this point, all test tubes have dye dissolved in toluene (200 μL). To all test tubes were added 2 mL of acetone to dissolve the toluene and dye (total volume 2.2 mL). The absorbance of each of these samples was measured by UV-Vis. Partition coefficients are reported as the ratio between the fluorous absorbance and the organic absorbance. All absorbance values were taken at the λ_{max} on a solvent/solvent basis.

Solubility limits. To 2 dram vials, dyes were deposited. Once dry of solvent, the appropriate solvent (PFMC or acetone, 200 μL) was added. The solutions were sonicated for at least one hour, then allowed to settle for at least two hours. Aliquots (10 μL) were taken close to the surface of the saturated dye solutions and evaporated to dryness. The residue was dissolved in acetone (200 μL) and the optical density measured. The concentration of dye in solution was determined using Beer's law. The relative solubility limits were calculated by normalizing to the least soluble dye (lowest concentration). All measurements were performed in duplicate.

Photophysical measurements (Figure 3D-H)

Instrumentation: Absorption spectra were recorded on a Jasco V-770 spectrophotometer. Fluorescence spectra were measured with a Horiba Fluorometer PTI QM-400. Quartz cuvettes (1 cm or 0.33 cm) were used for absorbance and photoluminescence measurements.

Absorption coefficient measurement: The absorption coefficient is calculated according to Beer-Lambert's law and is reported as the mean value of three independent determinations, with standard deviation as error:

$$A = \varepsilon bc$$

where A is the absorbance, b is the path length, and c is the concentration. All masses are measured on a Sartorius MSE6.6S-000-DM Cubis Micro Balance. The first stock solution is prepared in 1 mL of solvent, measured by Hamilton syringe, and further diluted by Hamilton syringes. At least five concentrations are measured before determining the absorption coefficients.

Fluorescence quantum yield measurement: The fluorescence quantum yield Φ_F of a material is defined as follows:

$$\Phi = \frac{P_E}{P_A}$$

where P_E, P_A are the number of photons emitted and absorbed respectively. To determine absolute quantum yield, the number of photons absorbed and emitted are measured independently. The quantum yield measurements are performed with a Horiba petite integrating sphere. The spectra are measured with a Horiba fluorimeter PTI QM-400. The sample optical density is kept below 0.1 to avoid fluorescence quenching and reabsorption effects. The experimental setup is adjusted and tested on standard dyes. Emission spectra are baseline corrected. The emission background for the blank is normalized by the transmission ratio of the blank and sample at the excitation line.

All irradiation was performed with THORLabs LEDs with SM1P25-A lens. Power was supplied with a KORAD KD3005D Digital-control DC Power Supply. Power densities were measured with a THORLabs PM100D Handheld Optical Power and Energy Meter.

Photobleaching studies (Figure 3E)

Solutions of dye in ethanol or PFOB were prepared. An LED setup consisting of :

- For **3** and **1a**: THORLabs M530L3 (530 nm) LED with SM2F32-A lens at 90 mW cm^{-2}
- For **1b**: THORLabs M660L4 (660 nm) LED with SM2F32-B lens at 90 mW cm^{-2}
- For **1c**: THORLabs M780L3 (780 nm) LED with SM2F32-B lens at 85 mW cm^{-2}

Power was supplied with a KORAD KD3005D Digital-control DC Power Supply: 0-30 V, 0-5 A. Power densities were measured with a THORLabs PM100D optical power meter. Cuvettes were placed 11 cm from the edge of the lens.

Time points were taken consistently between 3 trials for each solvent and dye combination, with the exception of F_{86}Cy3 in EtOH (only 1 trial). Data are reported as photobleaching rates, calculated by taking the slope of natural log of absorbances. Precise slopes were calculated using the LINEST function in Excel. Error is the standard deviation of absorbance averages. An example plot of raw photobleaching data are provided below.

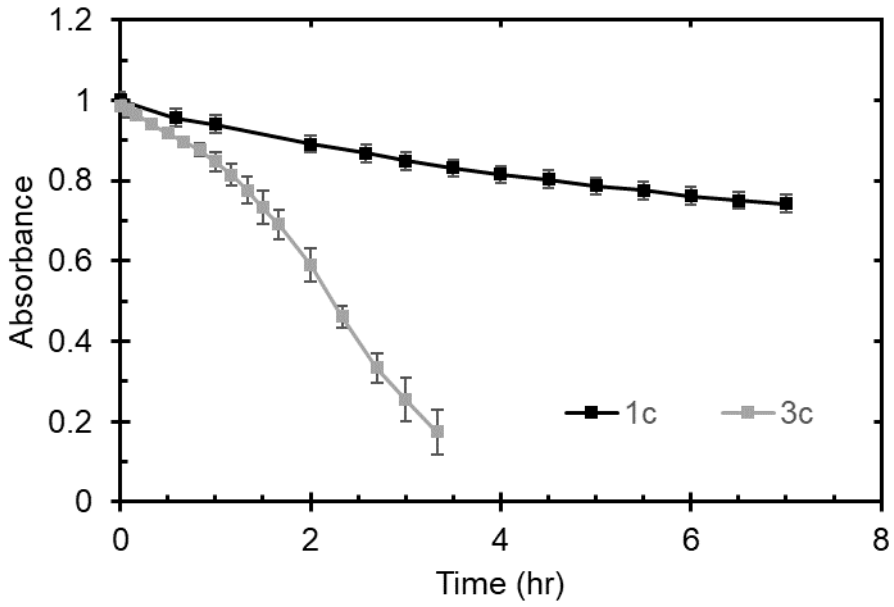

Figure S13: Raw photobleaching curves of heptamethine cyanines **1c** and **3c** in EtOH.

For air-free PFOB photobleaching rates, a solution of dye in PFOB was prepared first and freeze-pump-thawed (x3). This solution was carefully transferred to a nitrogen filled 1 cm quartz cuvette with a septum screw cap. The samples were immediately irradiated with light.

Corrections for photobleaching rates

In order to calculate the relative photobleaching rates (k_{rel}), the efficiency of absorption of the dyes in various solvents must be accounted for. Given a Gaussian distribution of emitted photons for each LED

(distribution provided by THORLabs), the areas under the curves were scaled to the measured power density according to equation 1 where I = photon density in mW cm^{-2} and P = Gaussian distribution.

$$I_s = I / \int_{270\,nm}^{1027\,nm} P \quad \text{Eq. 1}$$

The scaled integration of the LED was divided by the energy of the photon at each wavelength. Each wavelength is now accounted for the energy and the power density of the experimental setup (Eq. 2, 3).

$$E_p = \frac{hc}{\lambda} \quad \text{Eq. 2}$$

$$N_p = I_s / E_p \quad \text{Eq. 3}$$

$$X = \sum_{270\,nm}^{1027\,nm} N_p \times \sum_{270\,nm}^{1027\,nm} \varepsilon \quad \text{Eq. 4}$$

This is multiplied by the extinction coefficient of the dye in a particular solvent. The area under this convoluted curve is now the relative absorption efficiency of each dye in solvent, called the X factor (Eq. 4). X is multiplied by the raw rate of photobleaching to correct for absorption efficiency and the number of photons (Eq. 5).

$$k_{rel} = X \times k_{raw} \quad \text{Eq. 5}$$

The rates were further normalized by the fastest value to give factors of photobleaching, calculated in **Table S4**.

Table S4: Photobleaching corrections for each dye and solvent combination, according to the power density of the irradiating LED, absorbance coefficients of the dye in the solvent, and the number of photons reaching the dye in the cuvette. Freeze-pump-thawed (FPT) samples are displaced of oxygen.

Dye, Solvent	k_{raw}	**X factor**	k_{rel}	**Normalized**
1a, EtOH	0	2.30E-14	0	0
1a, PFOB	-0.035	4.92E-14	-1.72E-15	0.0052
1a, PFOB FPT	-0.00524	4.92E-14	-2.577E-16	0.00077
1b, PFOB	-2.7	2.04E-14	-5.49E-14	0.16
1c, EtOH	-0.0908	2.17E-13	-2.070E-14	0.059
1c, PFOB	-2.426	1.37E-13	-3.3318E-13	1
1c, PFOB FPT	-0.04793	1.37E-13	-6.5827E-15	0.020
3, EtOH	-0.009	5.43E-18	-4.9E-20	1.5E-07
3, PFOB	-0.041	4.56E-18	-2.4E-19	6.2E-07

Perfluorocarbon nanoemulsions (Figure 4)

General Nanoemulsion preparation procedure: Emulsions were prepared in a 1.5 mL Eppendorf tube using a QSonica (Q125) probe sonicator. A solution of dye in acetone (100 µL, 1.20 x10^{-4} M) was added to the bottom of an Eppendorf tube and the solvent was carefully evaporated with a gentle stream of nitrogen gas. Perfluorooctylbromide (PFOB) (20 µL) was added and the tube gently agitated to dissolve the dye (6.00 x10^{-4} M). A solution of Pluronic F-68 surfactant in PBS (200 µL, 28 mg mL^{-1}) was then layered on top of the PFOB solution. The tube was placed around the point of the probe sonicator, ensuring the probe was not in contact with the tube but fully submerged into the solution, then clamped and cooled with an ice bath. Immediately the sonicator was activated (35% amplitude, 90 sec). Upon completion, the Eppendorf was removed from the probe and used in further experiments.

Pluronic F-68 was chosen because of its clinical relevance and FDA-approval status. Additionally, this surfactant was chosen as the surfactant due to structure-property studies conducted in our lab. When comparing between diblock, triblock, fluorous-containing and non-fluorous hydrophobic blocks, the surfactant that best prevented leaching of the payload was Pluronic F-68.[2]

Emulsion partition (octanol/water) and leaching studies: An aliquot of dye-containing nanoemulsion solution (50 µL) was added to an Eppendorf tube (1.5 mL) containing PBS (950 µL). The solution was agitated by pipetting to ensure homogeneous suspension of the nanoemulsion. 1-octanol (500 µL) was then layered on top of the nanoemulsion in PBS solution. Sealed Eppendorf tubes were left on an orbital rocker (40 rotations/min), protected from light, at room temperature, for a set amount of time (1 h, 6 h, 1 d, 2 d, 4 d, 6 d). At each time point, an aliquot of the octanol layer (~200 µL) was removed from the tube, transferred to a quartz cuvette (3 mm), and the fluorescence spectrum was recorded with the following parameters (1 nm steps, 0.1 s integration time):

Dye in NE	Excitation λ (nm)	Excitation Slit Widths (nm)	Emission Collection Range (nm)	Emission Slit Widths (nm)
Rhodamine	500	2	520-700	2
F_{86}Cy3	520	3	540-750	3
F_{86}Cy5	600	3	620-815	3
F_{86}Cy7	700	5	725-900	5

Following characterization, the 1-octanol solution was returned to the Eppendorf tube and allowed to continue to rock, protected from light, until further time points.

The maximum fluorescence of each dye, equivalent to full leaching of dye contained within a 50 µL aliquot of nanoemulsion solution, was measured. A solution of dye in acetone (100 µL, 1.20 x10^{-4} M) was added to the bottom of an Eppendorf tube (1.5 mL) and the solvent was carefully evaporated with a gentle stream of nitrogen. PFOB (20 µL) was added and the tube agitated to dissolve the dye (6.00 x10^{-4} M). A portion of the dye in PFOB solution (4.5 µL, equivalent to the portion contained within a 50 µL aliquot of nanoemulsion prepared by the standard procedure listed in **Table S3**) was added to an Eppendorf tube containing 1-octanol saturated with PBS (500 µL) and sealed. The solution was well mixed with vigorous shaking, and a fluorescence spectrum recorded in a quartz cuvette (10 mm), using the same parameters as detailed above.

Leaching and partition of dye from the nanoemulsions into the 1-octanol layer was determined by the following equation:

$$\%\, Leached = \frac{Fluorescence\ at\ timepoint}{Maximum\ fluorescence} \quad \text{Eq. 6}$$

where the fluorescence is determined by the area under the curve in the emission spectrum. Data were collected in duplicate using two partitions for each dye.

Cellular microscopy and cytotoxicity studies

RAW264.7 cells were purchased from ATCC (Cat# TIB-71). RAW264.7 cells were cultured in Dulbecco's Modified Eagle Media (DMEM, Life Technologies, cat# 11995073) supplemented with 10% fetal bovine serum (Corning, lot# 35016109) and 1% penicillin-streptomycin (Life Technologies, cat# 15070063). Cells were washed with PBS, or PBS supplemented with 1% fetal bovine serum (FBS, FACS buffer). Cells were incubated at 37 ˚C, 5% CO_2, during treatments and throughout culturing, in HERACell 150i CO2 incubators. Cells were pelleted through use of Sorvall ST 40R centrifuge. All cell work was performed in 1300 Series A2 biosafety cabinets.

Pluronic F-68-stabilized emulsions were prepared as described by the general nanoemulsion formation procedure. After size and zeta potential measurements had been taken, emulsions were washed by centrifugation and suspension (3x, 5.6 *g* followed by resuspension in 100 µL PBS). On the last wash, emulsions were resuspended in PBS buffer (100 µL).

For cell viability experiments: following incubation, cells were washed three times by centrifugation (526 x *g*, 3 min, 4 ˚C). Propidium iodide solution (2 µL in 1 mg/mL in PBS) was added to each well. Cells/PI were transferred to FACS tubes with a final volume of 200 µL FACS buffer (PBS + 1% FBS). Cells were incubated on ice for 15 minutes prior to flow cytometry measurement. PI fluorescence was measured on FL2 channel. Data were analyzed by splitting the population at 10^2 as a live/dead line. Flow cytometry was performed on a BDBiosciences FACSCalibur equipped with 488 nm and 635 nm lasers. For assessment of the statistical significance of differences, a one-tailed Student's t-test assuming unequal sample variance was employed. Results were considered significant/not significant per the following definitions: ns = $p > 0.05$, significant = $p < 0.05$, * = $p \leq 0.05$, ** = $p \leq 0.01$, *** = $p \leq 0.001$.

For microscopy experiments: RAW264.7 cells (20,000 cells/well) were plated on a µ-Slide 8 Well ibiTreat tissue culture treated slides (Ibidi Cat# 80826). Cells were allowed to adhere overnight. Media was replaced with complete DMEM and treated with emulsions (40 µL). Treatment was incubated for 3 h (37 ˚C, 5% CO_2). After treatment, cells were washed with media 3x, LiCl buffer 3x and replaced with OptiMEM containing cellular stains. PFOB emulsions are dense and settle onto the cells. To remove the emulsions, slight rocking was necessary. Cells were stained with Hoechst (3.24 µM, ThermoFisher Cat# PI62249), Mitotracker green (20 nM, Cell Signaling Technologies Cat# 9074S) and Lysotracker red (25 nM, Cell Signaling Technologies Cat# L7528) in OptiMEM. Cells were incubated with Hoescht at room temperature for 30 minutes prior to imaging, Hoescht in OptiMEM was removed and replaced with OptiMEM containing LysoTracker stains and imaged immediately.

Confocal microscopy was performed on a TCS SPE Leica confocal microscope containing 405 nm, 488 nm, 532 nm and 635 nm lasers. Hoechst (405 laser-50%, 800 gain, offset -0.4, collection 420-500nm), green stains (488 laser-50%, 800 gain, offset -0.4, collection 500-550 nm), red stains (532 laser-50%, 800 gain, offset -0.4, collection 540-700nm), deep red stains (635 laser-50%, 800 gain, offset -0.4, collection 540-700nm), DIC (scan-BF, 450 gain, offset -0.4). Scale bar represents 7.5 µm. Images were processed in ImageJ.

Measurements of cellular forces with microdroplets in zebrafish embryos and multicellular spheroids (Figure 5)

Zebrafish husbandry, transgenic lines and experimental manipulations

Zebrafish (*Danio rerio*) were maintained under standard conditions.[2] Animal husbandry and experiments were done according to protocols approved by the Institutional Animal Care and Use Committee (IACUC) at the University of California Santa Barbara. Double transgenic lines Tg(h2afva:eGFP)^{kca6} x Tg(actb2:memCherry2)^{hm29} double transgenic embryos were used to visualize nuclei and membranes respectively. Fluorinated droplets were inserted in zebrafish embryos through direct injection of the fluorinated oil (containing Krytox-PEG(600) and a fluorinated dye, as described in the main text) in the tissue of interest at the 4-6 somite stage, as previously described.[3] Droplets were imaged at least 2h after injection to enable enough time for the tissue to recover, as previously done.[4,5]

Imaging

In all cases, 8-10 somite stage zebrafish embryos were mounted in 1% low-melting point agarose in a glass bottom petri dish (MatTek Corporation) for a dorsal view of the tailbud and imaged at 25 ºC using a 40x water immersion objective (LD C-Apochromat 1.1 W, Carl Zeiss) on an inverted Zeiss Laser Scanning Confocal (LSM 710, Carl Zeiss Inc.). To observe the mCherry labelled cell membranes (Tg(actb2:memCherry2)^{hm29}), a 594 nm laser line was used as excitation source and the selected emission spectral window was set to 599-697 nm. For the observation of the GFP-labelled nuclei (Tg(h2afva:eGFP)^{kca6}), a 488 nm laser line was used as excitation source and the selected emission spectral window was set to 493-574 nm. Rhodamine **3** and F_{86}Cy5 **1b** labelled droplets were excited with 543 nm and 633 nm laser lines, respectively. The selected emission spectral windows were set to 548-598 nm and 652-759 nm to observe Rhodamine and F_{86}Cy5, respectively.

Interfacial tension measurements

In order to obtain quantify the mechanical stresses in biological tissues with oil microdroplets, it is necessary to know the droplet interfacial tension.[6] The interfacial tension of fluorinated droplets (HFE-7700, 3M) was controlled using a fluorinated surfactant, Krytox-PEG(600) (KP600, Ran Biotech), as previously described.[7] To understand the effect of the fluorinated dyes the droplet interfacial tension, we measured the interfacial tension of droplets in the presence and absence of fluorinated dyes (Figure S14). Specifically, we prepared solutions of 0.25 mM Rhodamine **3**, F_{86}Cy3 **1a** and F_{86}Cy5 **1b** either with or without fluorinated surfactant (2 wt% Krytox-PEG(600)) in HFE-7700 and measured their interfacial tension in water using a pendant drop tensiometer (Biolin Scientific). In the absence of Krytox-PEG(600), the interfacial tension is reduced by varying amount depending of the dye (Figure S14), indicating that the dyes act as surfactants. This is consistent with their localization of the droplet surface in the absence of Krytox-PEG(600). However, in the presence of Krytox-PEG(600), the interfacial tension is controlled by the fluorinated surfactant. The fluorinated dyes do not alter significantly the interfacial tension set by the surfactant and they do not localize at the surface (Figure S14), indicating that the surfactant controls the interfacial properties. While the presence of the new F_{86}Cy3 and F_{86}Cy5 dyes does not affect the interfacial tension if Krytox-PEG(600) is present, Rhodamine **3** does increase slightly the droplet interfacial tension (approximately by 25-30%; Figure S14).

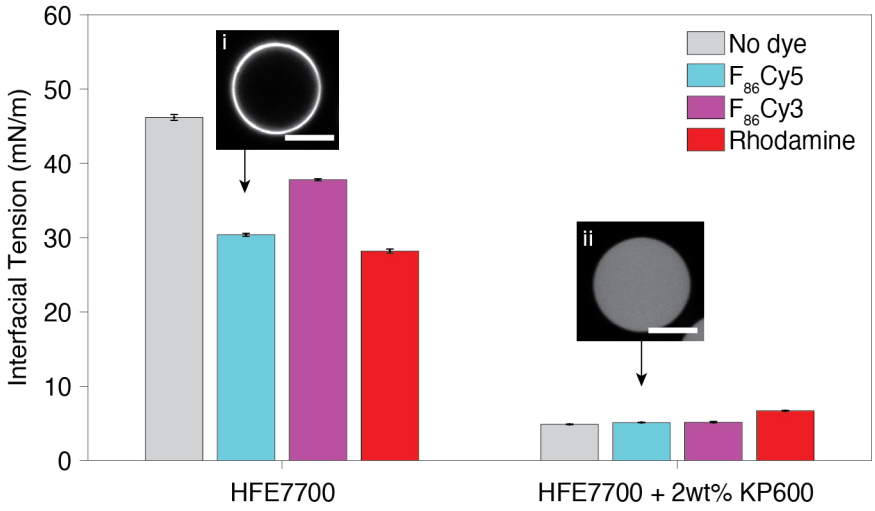

Figure S14: Interfacial tension measurements of fluorinated dyes diluted in HFE-7700 in the presence and absence of fluorinated surfactant (2 wt% Krytox-PEG(600)). In each case, four conditions were tested: no dye, 0.025 mM Rhodamine, 0.025 mM F_{86}Cy3 and 0.025 mM F_{86}Cy5. The insets show confocal sections of droplets containing 0.025 mM F_{86}Cy5 in HFE-7700, both in the absence (i) and presence (ii) of Krytox-PEG(600). Scale bars, 10 μm.

Since the values of interfacial tension needed for force measurements with droplets are those of droplets in cell culture media, rather than water, we measured the values of interfacial tension of the different solutions containing the different fluorinated dyes in cell culture media. Comparison of the measured values to those in water (Figure S15) shows that the interfacial tension of the different solutions is essentially the same in water than in cell culture media and is controlled by the presence of the fluorinated surfactant Krytox-PEG(600).

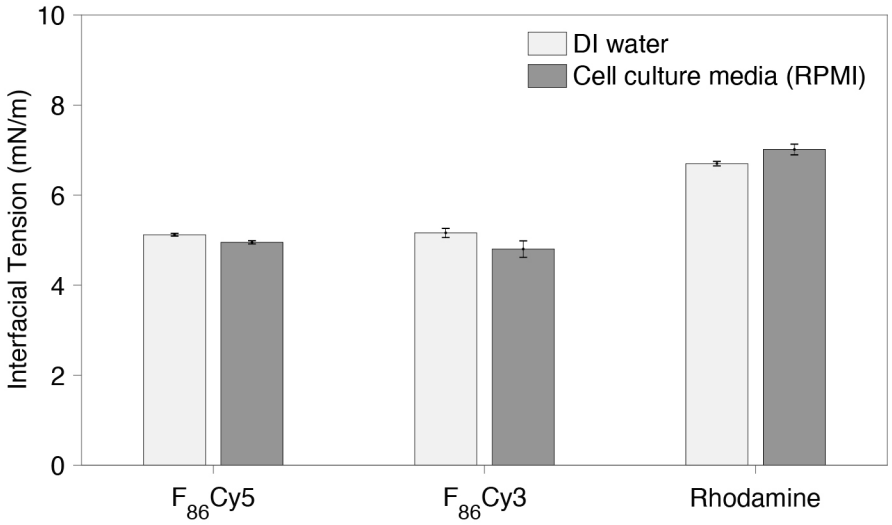

Figure S15: Comparison of interfacial tension measurements of fluorinated dyes diluted in HFE-7700 (with 2 wt% Krytox-PEG(600)) in water and in cell culture media. The interfacial tension in cell culture media is essentially the same as in water and it is controlled by the presence of a fluorinated surfactant Krytox-PEG(600).

Multicellular spheroid formation and experimental manipulations

Mouse 4T1 breast cancer cells were maintained at 37 ºC and 5% CO_2 in RPMI 1630 Medium supplemented with 10% fetal bovine serum (FBS) and 1% Penicillin Streptomycin (PenStrep). To visualize the nuclei, cells were transfected with GFP-NLS using a lentivirus (Essen Bioscience, 4475). Transfected cells were selected using puromycin-containing cell culture media (1 μg ml^{-1}; Thermo Fisher, A1113802). Spheroids of these transfected cells were prepared using the hanging drop method.[8] In order to make spheroids with a diameter of approximately 150 μm, we placed about 100 cells per 5 μL drop and incubated the 3D culture for 3 days. These spheroids were injected with HFE-7700 oil (containing 2% Krytox-PEG(600) surfactant and 0.025 mM of either F_{86}Cy5 **1b** or Rhodamine **3**) using a pressure-controlled microinjector (droplet size controlled by changing pressure and time of injection), and incubated for an additional 24 hours after injection.

Imaging of multicellular spheroids

Spheroids containing droplets were transferred to a glass-bottom microwell dish (MatTek) and mounted in 2% agarose for imaging. The dishes were supplemented with 2 mL of cell culture media. A laser scanning confocal (LSM710, Carl Zeiss Inc.) equipped with a 25x water immersion objective and an incubation chamber (maintained at 37 ºC and 5% CO_2) was used to image the samples. Imaging of cells (GFP labelled nuclei) and droplets (either F_{86}Cy5 **1b** or Rhodamine **3**) was done on separate tracks using excitation lasers at 488 nm and 543nm (for Rhodamine **3**) or 633 nm (for F_{86}Cy5), respectively.

Droplet reconstruction

Droplet 3D surface reconstruction and analysis of the droplet deformations were done as previously described.[8] Briefly, the surface of the droplet is located, described by a point cloud and the map of mean curvature H on the droplet surface is calculated from the point cloud. The anisotropic stresses σ_{nn}^{A} are directly obtained from the mean curvature map and the interfacial tension γ, namely $\sigma_{nn}^{A} = \gamma(H - H_0)$, where H_0 is the average mean curvature of the droplet.[5,6] To map the anisotropic mechanical stresses on the droplet surface for droplets in multicellular spheroids, we used the values of interfacial tension measured for droplets (containing a specific dye) in cell culture media (Figure S15).

Crystallographic information

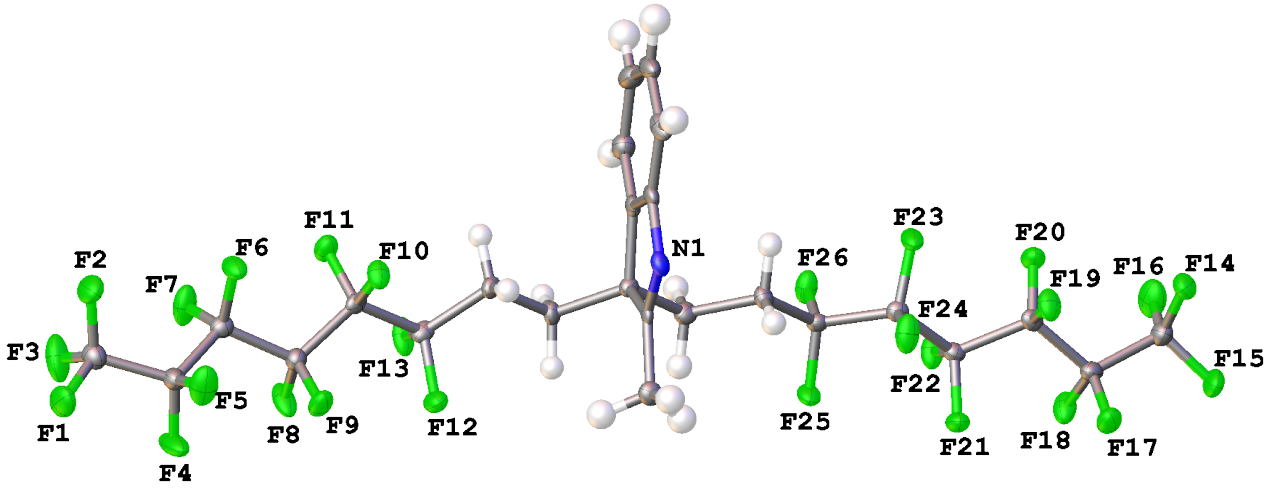

Table S5. Crystal data and structure refinement for indole **9**.

Identification code	IL-III-188-263A	
Empirical formula	C25 H15 F26 N	
Formula weight	823.38	
Temperature	100.0 K	
Wavelength	0.71073 Å	
Crystal system	Triclinic	
Space group	P-1	
Unit cell dimensions	a = 11.2473(19) Å	α = 71.197(6)°.
	b = 12.2989(14) Å	β = 67.507(4)°.
	c = 12.6264(18) Å	γ = 70.565(4)°.
Volume	1483.2(4) $Å^3$	
Z	2	
Density (calculated)	1.844 Mg/m^3	
Absorption coefficient	0.223 mm^{-1}	
F(000)	812	
Crystal size	0.34 x 0.33 x 0.31 mm^3	
Theta range for data collection	1.791 to 25.362°.	
Index ranges	-9<=h<=13, -14<=k<=14, -15<=l<=15	
Reflections collected	17033	
Independent reflections	5426 [R(int) = 0.0357]	
Completeness to theta = 25.242°	99.9 %	
Absorption correction	Semi-empirical from equivalents	
Max. and min. transmission	0.7452 and 0.6842	
Refinement method	Full-matrix least-squares on F^2	
Data / restraints / parameters	5426 / 0 / 470	
Goodness-of-fit on F^2	1.009	
Final R indices [I>2sigma(I)]	R1 = 0.0374, wR2 = 0.0775	
R indices (all data)	R1 = 0.0607, wR2 = 0.0867	

Extinction coefficient	n/a
Largest diff. peak and hole	0.404 and -0.305 e.Å^{-3}

Table S6. Atomic coordinates (x 10^4) and equivalent isotropic displacement parameters (Å^{2}x 10^3) for indole **9**. U(eq) is defined as one third of the trace of the orthogonalized U^{ij} tensor.

	x	y	z	U(eq)
F(10)	9606(1)	2172(1)	4539(1)	24(1)
F(26)	3829(1)	8480(1)	7940(1)	27(1)
F(6)	10220(1)	212(1)	3767(1)	30(1)
F(20)	3448(1)	11109(1)	9574(1)	26(1)
F(22)	3009(1)	10794(1)	7833(1)	29(1)
F(25)	4700(1)	9424(1)	6160(1)	29(1)
F(14)	3760(1)	13241(1)	9840(1)	33(1)
F(11)	7839(1)	1508(1)	5108(1)	26(1)
F(23)	5138(1)	9171(1)	8821(1)	31(1)
F(12)	7968(1)	4341(1)	3388(1)	29(1)
F(13)	6338(1)	3540(1)	4587(1)	32(1)
F(19)	5367(1)	11493(1)	8494(1)	28(1)
F(21)	4614(1)	11573(1)	6522(1)	31(1)
F(17)	4351(1)	13500(1)	7363(1)	32(1)
F(9)	9809(1)	2656(1)	2326(1)	32(1)
F(18)	2455(1)	13087(1)	7809(1)	33(1)
F(16)	1788(1)	13225(1)	10000(1)	42(1)
F(15)	2614(2)	14695(1)	8865(1)	40(1)
F(2)	11225(1)	-1532(1)	2484(1)	38(1)
F(8)	7832(1)	2444(1)	2692(1)	36(1)
F(24)	6436(1)	9833(1)	7100(1)	34(1)
F(1)	11619(2)	-860(1)	621(1)	41(1)
F(7)	8484(1)	188(1)	3417(1)	37(1)
F(4)	9785(2)	1213(1)	1007(1)	51(1)
F(5)	11526(2)	772(1)	1573(1)	42(1)
F(3)	9678(2)	-1070(1)	1712(2)	48(1)
N(1)	9115(2)	5676(2)	6212(2)	20(1)
C(23)	6931(2)	5812(2)	6271(2)	16(1)
C(9)	9486(2)	717(2)	3034(2)	20(1)
C(18)	5206(2)	9673(2)	7688(2)	18(1)
C(17)	4958(2)	8801(2)	7188(2)	18(1)

C(24)	8278(2)	6118(2)	5624(2)	17(1)
C(22)	2886(2)	13531(2)	9259(2)	26(1)
C(19)	4229(2)	10914(2)	7619(2)	18(1)
C(1)	7177(2)	5052(2)	7411(2)	18(1)
C(8)	10372(2)	505(2)	1811(2)	24(1)
C(6)	8458(2)	5011(2)	7325(2)	19(1)
C(7)	10724(2)	-775(2)	1656(2)	26(1)
C(20)	4143(2)	11594(2)	8498(2)	18(1)
C(12)	7598(2)	3566(2)	4435(2)	19(1)
C(13)	7648(2)	3980(2)	5410(2)	18(1)
C(16)	6084(2)	7731(2)	7000(2)	20(1)
C(11)	8486(2)	2319(2)	4296(2)	17(1)
C(21)	3461(2)	12933(2)	8213(2)	22(1)
C(10)	8896(2)	2055(2)	3075(2)	20(1)
C(5)	8984(2)	4386(2)	8243(2)	27(1)
C(14)	6623(2)	5150(2)	5591(2)	18(1)
C(15)	5799(2)	6932(2)	6460(2)	19(1)
C(25)	8592(2)	6871(2)	4413(2)	22(1)
C(4)	8177(3)	3793(2)	9252(2)	31(1)
C(2)	6378(2)	4475(2)	8425(2)	25(1)
C(3)	6899(3)	3833(2)	9348(2)	31(1)

Table S7. Bond lengths [Å] and angles [°] for indole **9**.

Bond lengths		Bond angles	
F(10)-C(11)	1.350(2)	C(24)-N(1)-C(6)	106.42(18)
F(26)-C(17)	1.357(2)	C(24)-C(23)-C(14)	111.40(17)
F(6)-C(9)	1.341(2)	C(24)-C(23)-C(15)	111.58(16)
F(20)-C(20)	1.337(2)	C(1)-C(23)-C(24)	99.43(16)
F(22)-C(19)	1.343(2)	C(1)-C(23)-C(14)	113.64(16)
F(25)-C(17)	1.361(2)	C(1)-C(23)-C(15)	112.21(17)
F(14)-C(22)	1.334(3)	C(14)-C(23)-C(15)	108.44(17)
F(11)-C(11)	1.353(2)	F(6)-C(9)-C(8)	107.68(17)
F(23)-C(18)	1.346(2)	F(6)-C(9)-C(10)	108.63(17)
F(12)-C(12)	1.363(2)	F(7)-C(9)-F(6)	108.26(16)
F(13)-C(12)	1.365(2)	F(7)-C(9)-C(8)	109.48(18)
F(19)-C(20)	1.339(2)	F(7)-C(9)-C(10)	108.63(17)
F(21)-C(19)	1.346(2)	C(8)-C(9)-C(10)	114.02(17)
F(17)-C(21)	1.341(2)	F(23)-C(18)-C(17)	107.87(16)
F(9)-C(10)	1.344(2)	F(23)-C(18)-C(19)	108.79(16)
F(18)-C(21)	1.347(3)	F(24)-C(18)-F(23)	108.06(17)
F(16)-C(22)	1.320(3)	F(24)-C(18)-C(17)	109.04(17)
F(15)-C(22)	1.325(2)	F(24)-C(18)-C(19)	107.50(16)
F(2)-C(7)	1.324(3)	C(17)-C(18)-C(19)	115.38(17)
F(8)-C(10)	1.344(2)	F(26)-C(17)-F(25)	106.63(16)
F(24)-C(18)	1.344(2)	F(26)-C(17)-C(18)	107.31(16)
F(1)-C(7)	1.321(3)	F(26)-C(17)-C(16)	110.71(17)
F(7)-C(9)	1.339(2)	F(25)-C(17)-C(18)	106.88(16)
F(4)-C(8)	1.336(3)	F(25)-C(17)-C(16)	110.92(17)
F(5)-C(8)	1.343(3)	C(16)-C(17)-C(18)	114.02(18)
F(3)-C(7)	1.313(3)	N(1)-C(24)-C(23)	114.82(18)
N(1)-C(24)	1.291(3)	N(1)-C(24)-C(25)	122.8(2)
N(1)-C(6)	1.434(3)	C(25)-C(24)-C(23)	122.40(18)
C(23)-C(24)	1.528(3)	F(14)-C(22)-C(21)	110.75(18)
C(23)-C(1)	1.511(3)	F(16)-C(22)-F(14)	108.62(18)
C(23)-C(14)	1.546(3)	F(16)-C(22)-F(15)	108.60(19)
C(23)-C(15)	1.546(3)	F(16)-C(22)-C(21)	111.49(19)

C(9)-C(8)	1.535(3)	F(15)-C(22)-F(14)	108.14(19)
C(9)-C(10)	1.566(3)	F(15)-C(22)-C(21)	109.17(18)
C(18)-C(17)	1.547(3)	F(22)-C(19)-F(21)	108.37(17)
C(18)-C(19)	1.555(3)	F(22)-C(19)-C(18)	109.14(16)
C(17)-C(16)	1.502(3)	F(22)-C(19)-C(20)	107.89(16)
C(24)-C(25)	1.488(3)	F(21)-C(19)-C(18)	108.65(17)
C(22)-C(21)	1.537(3)	F(21)-C(19)-C(20)	108.35(16)
C(19)-C(20)	1.550(3)	C(20)-C(19)-C(18)	114.29(17)
C(1)-C(6)	1.388(3)	C(6)-C(1)-C(23)	107.38(18)
C(1)-C(2)	1.382(3)	C(2)-C(1)-C(23)	132.1(2)
C(8)-C(7)	1.548(3)	C(2)-C(1)-C(6)	120.5(2)
C(6)-C(5)	1.390(3)	F(4)-C(8)-F(5)	108.88(18)
C(20)-C(21)	1.555(3)	F(4)-C(8)-C(9)	109.43(18)
C(12)-C(13)	1.500(3)	F(4)-C(8)-C(7)	107.38(18)
C(12)-C(11)	1.549(3)	F(5)-C(8)-C(9)	108.33(18)
C(13)-H(13A)	0.9900	F(5)-C(8)-C(7)	106.59(18)
C(13)-H(13B)	0.9900	C(9)-C(8)-C(7)	116.02(18)
C(13)-C(14)	1.535(3)	C(1)-C(6)-N(1)	111.95(18)
C(16)-H(16A)	0.9900	C(1)-C(6)-C(5)	121.6(2)
C(16)-H(16B)	0.9900	C(5)-C(6)-N(1)	126.5(2)
C(16)-C(15)	1.531(3)	F(2)-C(7)-C(8)	110.31(19)
C(11)-C(10)	1.542(3)	F(1)-C(7)-F(2)	108.51(19)
C(5)-H(5)	0.9500	F(1)-C(7)-C(8)	109.23(18)
C(5)-C(4)	1.391(3)	F(3)-C(7)-F(2)	108.53(19)
C(14)-H(14A)	0.9900	F(3)-C(7)-F(1)	108.6(2)
C(14)-H(14B)	0.9900	F(3)-C(7)-C(8)	111.56(19)
C(15)-H(15A)	0.9900	F(20)-C(20)-F(19)	109.13(17)
C(15)-H(15B)	0.9900	F(20)-C(20)-C(19)	108.49(16)
C(25)-H(25A)	0.9800	F(20)-C(20)-C(21)	108.20(17)
C(25)-H(25B)	0.9800	F(19)-C(20)-C(19)	109.20(16)
C(25)-H(25C)	0.9800	F(19)-C(20)-C(21)	108.14(17)
C(4)-H(4)	0.9500	C(19)-C(20)-C(21)	113.61(17)
C(4)-C(3)	1.380(4)	F(12)-C(12)-F(13)	105.82(16)
C(2)-H(2)	0.9500	F(12)-C(12)-C(13)	110.07(17)
C(2)-C(3)	1.395(3)	F(12)-C(12)-C(11)	107.71(17)

C(3)-H(3)	0.9500	F(13)-C(12)-C(13)	111.30(17)
		F(13)-C(12)-C(11)	106.79(16)
		C(13)-C(12)-C(11)	114.69(17)
		C(12)-C(13)-H(13A)	109.3
		C(12)-C(13)-H(13B)	109.3
		C(12)-C(13)-C(14)	111.68(17)
		H(13A)-C(13)-H(13B)	107.9
		C(14)-C(13)-H(13A)	109.3
		C(14)-C(13)-H(13B)	109.3
		C(17)-C(16)-H(16A)	109.4
		C(17)-C(16)-H(16B)	109.4
		C(17)-C(16)-C(15)	111.34(18)
		H(16A)-C(16)-H(16B)	108.0
		C(15)-C(16)-H(16A)	109.4
		C(15)-C(16)-H(16B)	109.4
		F(10)-C(11)-F(11)	107.41(16)
		F(10)-C(11)-C(12)	108.67(16)
		F(10)-C(11)-C(10)	107.61(16)
		F(11)-C(11)-C(12)	108.15(16)
		F(11)-C(11)-C(10)	108.69(16)
		C(10)-C(11)-C(12)	116.00(17)
		F(17)-C(21)-F(18)	108.18(17)
		F(17)-C(21)-C(22)	108.19(17)
		F(17)-C(21)-C(20)	108.59(18)
		F(18)-C(21)-C(22)	107.06(18)
		F(18)-C(21)-C(20)	109.71(17)
		C(22)-C(21)-C(20)	114.91(18)
		F(9)-C(10)-C(9)	108.17(17)
		F(9)-C(10)-C(11)	108.34(17)
		F(8)-C(10)-F(9)	108.28(17)
		F(8)-C(10)-C(9)	107.91(17)
		F(8)-C(10)-C(11)	109.01(17)
		C(11)-C(10)-C(9)	114.95(17)
		C(6)-C(5)-H(5)	121.4
		C(6)-C(5)-C(4)	117.3(2)

C(4)-C(5)-H(5)	121.4
C(23)-C(14)-H(14A)	109.0
C(23)-C(14)-H(14B)	109.0
C(13)-C(14)-C(23)	113.12(17)
C(13)-C(14)-H(14A)	109.0
C(13)-C(14)-H(14B)	109.0
H(14A)-C(14)-H(14B)	107.8
C(23)-C(15)-H(15A)	109.1
C(23)-C(15)-H(15B)	109.1
C(16)-C(15)-C(23)	112.69(17)
C(16)-C(15)-H(15A)	109.1
C(16)-C(15)-H(15B)	109.1
H(15A)-C(15)-H(15B)	107.8
C(24)-C(25)-H(25A)	109.5
C(24)-C(25)-H(25B)	109.5
C(24)-C(25)-H(25C)	109.5
H(25A)-C(25)-H(25B)	109.5
H(25A)-C(25)-H(25C)	109.5
H(25B)-C(25)-H(25C)	109.5
C(5)-C(4)-H(4)	119.2
C(3)-C(4)-C(5)	121.6(2)
C(3)-C(4)-H(4)	119.2
C(1)-C(2)-H(2)	120.8
C(1)-C(2)-C(3)	118.5(2)
C(3)-C(2)-H(2)	120.8
C(4)-C(3)-C(2)	120.5(2)
C(4)-C(3)-H(3)	119.7
C(2)-C(3)-H(3)	119.7

Table S8. Anisotropic displacement parameters ($Å^2 x\ 10^3$) for indole **9**. The anisotropic displacement factor exponent takes the form: $-2\pi^2[\ h^2\ a^{*2}U^{11} + ... + 2\ h\ k\ a^*\ b^*\ U^{12}\ ]$

	U^{11}	U^{22}	U^{33}	U^{23}	U^{13}	U^{12}
F(10)	22(1)	23(1)	34(1)	-13(1)	-17(1)	2(1)
F(26)	21(1)	25(1)	37(1)	-14(1)	-1(1)	-8(1)
F(6)	42(1)	22(1)	24(1)	-7(1)	-20(1)	6(1)
F(20)	38(1)	21(1)	17(1)	-3(1)	-4(1)	-9(1)
F(22)	22(1)	25(1)	49(1)	-18(1)	-18(1)	0(1)
F(25)	46(1)	21(1)	25(1)	-5(1)	-23(1)	0(1)
F(14)	53(1)	29(1)	27(1)	-8(1)	-21(1)	-9(1)
F(11)	31(1)	20(1)	25(1)	-5(1)	-2(1)	-10(1)
F(23)	52(1)	19(1)	26(1)	-6(1)	-26(1)	3(1)
F(12)	47(1)	16(1)	22(1)	-3(1)	-15(1)	-1(1)
F(13)	20(1)	33(1)	54(1)	-25(1)	-20(1)	2(1)
F(19)	25(1)	29(1)	39(1)	-14(1)	-17(1)	-3(1)
F(21)	54(1)	20(1)	17(1)	-2(1)	-13(1)	-6(1)
F(17)	49(1)	23(1)	23(1)	-2(1)	-5(1)	-16(1)
F(9)	48(1)	19(1)	23(1)	-4(1)	0(1)	-12(1)
F(18)	40(1)	22(1)	47(1)	-13(1)	-31(1)	4(1)
F(16)	37(1)	38(1)	43(1)	-21(1)	4(1)	-8(1)
F(15)	70(1)	17(1)	34(1)	-9(1)	-24(1)	-1(1)
F(2)	53(1)	20(1)	36(1)	-8(1)	-20(1)	4(1)
F(8)	40(1)	33(1)	47(1)	-23(1)	-34(1)	13(1)
F(24)	20(1)	32(1)	54(1)	-23(1)	-6(1)	-6(1)
F(1)	56(1)	32(1)	27(1)	-16(1)	0(1)	-5(1)
F(7)	30(1)	32(1)	52(1)	-23(1)	2(1)	-15(1)
F(4)	89(1)	30(1)	29(1)	-11(1)	-35(1)	17(1)
F(5)	40(1)	37(1)	43(1)	-19(1)	11(1)	-20(1)
F(3)	39(1)	49(1)	75(1)	-42(1)	-19(1)	-6(1)
N(1)	20(1)	22(1)	20(1)	-9(1)	-7(1)	-3(1)
C(23)	16(1)	17(1)	18(1)	-4(1)	-8(1)	-4(1)
C(9)	20(1)	18(1)	21(1)	-2(1)	-7(1)	-5(1)
C(18)	18(1)	20(1)	18(1)	-3(1)	-7(1)	-5(1)
C(17)	21(1)	19(1)	15(1)	-2(1)	-7(1)	-6(1)

C(24)	18(1)	14(1)	20(1)	-9(1)	-6(1)	-2(1)
C(22)	35(2)	19(1)	24(1)	-5(1)	-10(1)	-5(1)
C(19)	19(1)	20(1)	16(1)	-3(1)	-7(1)	-6(1)
C(1)	20(1)	15(1)	19(1)	-9(1)	-7(1)	0(1)
C(8)	33(2)	19(1)	20(1)	-3(1)	-11(1)	-3(1)
C(6)	23(1)	19(1)	18(1)	-10(1)	-9(1)	1(1)
C(7)	29(1)	24(1)	25(1)	-9(1)	-10(1)	-3(1)
C(20)	18(1)	21(1)	16(1)	-3(1)	-6(1)	-8(1)
C(12)	16(1)	17(1)	25(1)	-3(1)	-11(1)	-3(1)
C(13)	19(1)	17(1)	23(1)	-6(1)	-10(1)	-3(1)
C(16)	21(1)	20(1)	23(1)	-8(1)	-10(1)	-3(1)
C(11)	16(1)	17(1)	22(1)	-3(1)	-9(1)	-7(1)
C(21)	29(1)	20(1)	20(1)	-3(1)	-11(1)	-7(1)
C(10)	21(1)	19(1)	21(1)	-4(1)	-9(1)	-3(1)
C(5)	27(1)	28(1)	28(1)	-14(1)	-16(1)	6(1)
C(14)	18(1)	17(1)	22(1)	-7(1)	-9(1)	-3(1)
C(15)	18(1)	19(1)	22(1)	-7(1)	-9(1)	-2(1)
C(25)	23(1)	25(1)	21(1)	-4(1)	-7(1)	-7(1)
C(4)	46(2)	21(1)	21(1)	-7(1)	-17(1)	5(1)
C(2)	29(1)	24(1)	22(1)	-7(1)	-5(1)	-8(1)
C(3)	47(2)	20(1)	21(1)	-4(1)	-6(1)	-7(1)

Table S9. Hydrogen coordinates (x 10^4) and isotropic displacement parameters ($Å^2$x 10^3) for indole **9**.

	x	y	z	U(eq)
H(13A)	8546	4088	5223	22
H(13B)	7476	3368	6149	22
H(16A)	6231	7279	7763	24
H(16B)	6904	7986	6473	24
H(5)	9859	4364	8184	32
H(14A)	5737	4985	6027	22
H(14B)	6591	5668	4813	22
H(15A)	5660	7386	5695	23
H(15B)	4969	6692	6984	23
H(25A)	9445	7060	4207	34
H(25B)	7896	7605	4377	34
H(25C)	8643	6445	3855	34
H(4)	8513	3349	9890	37
H(2)	5494	4515	8493	30
H(3)	6370	3420	10048	37

Nuclear magnetic resonance spectra

^{1}H NMR (300 MHz, $CDCl_3$) **S7**

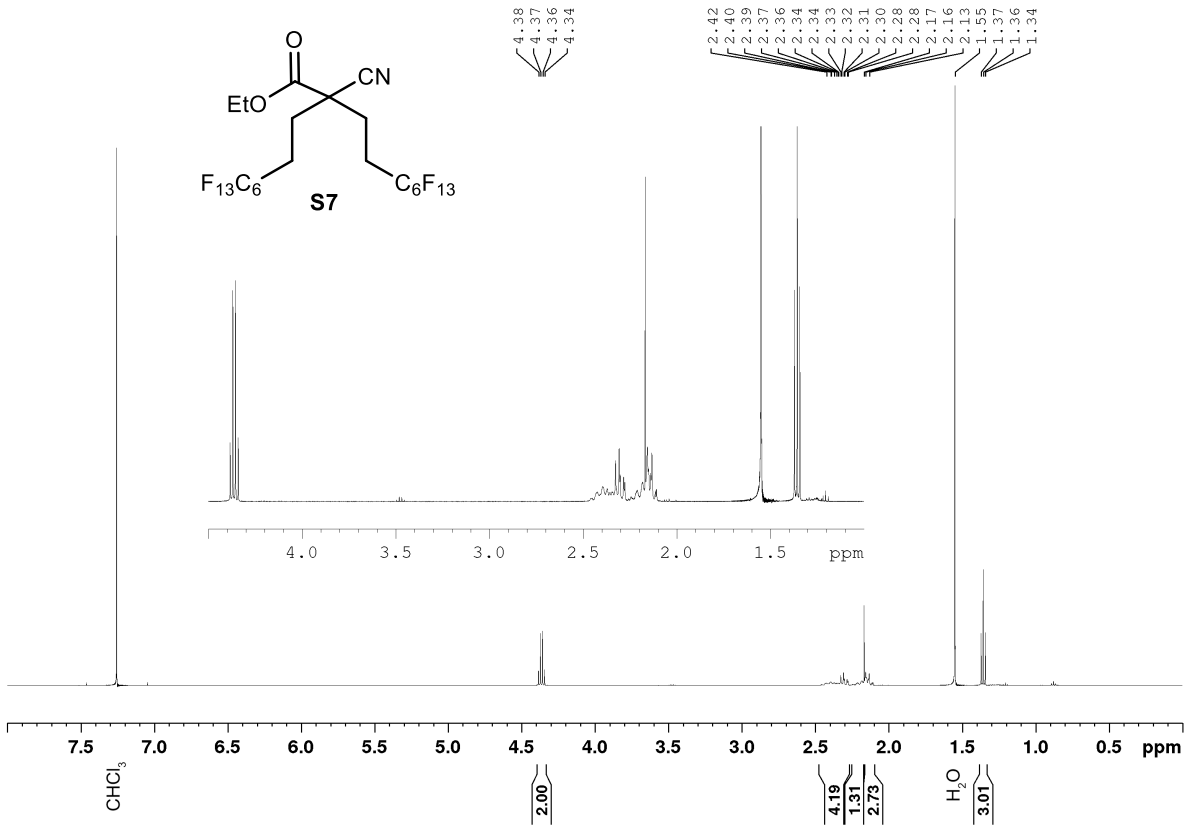

^{1}H NMR (300 MHz, $CDCl_3$) **7**

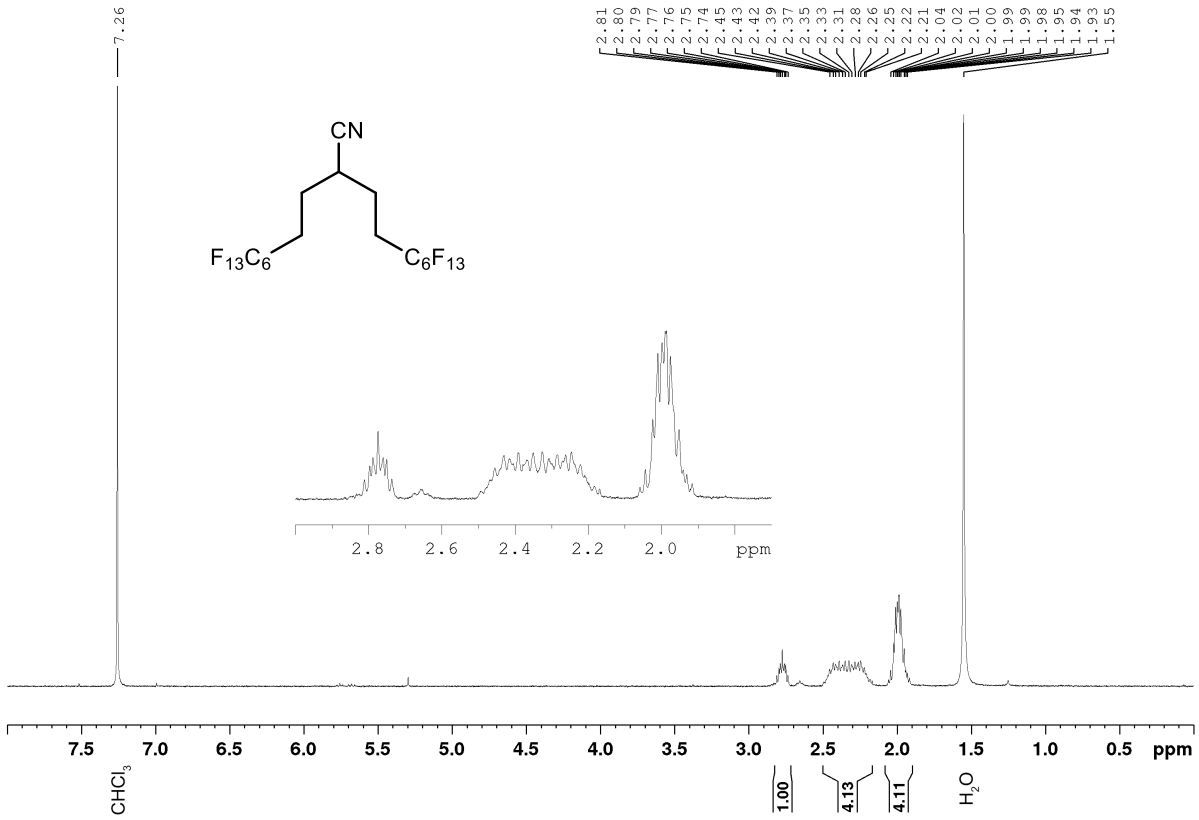

^{1}H NMR (300 MHz, $CDCl_3$) **8**

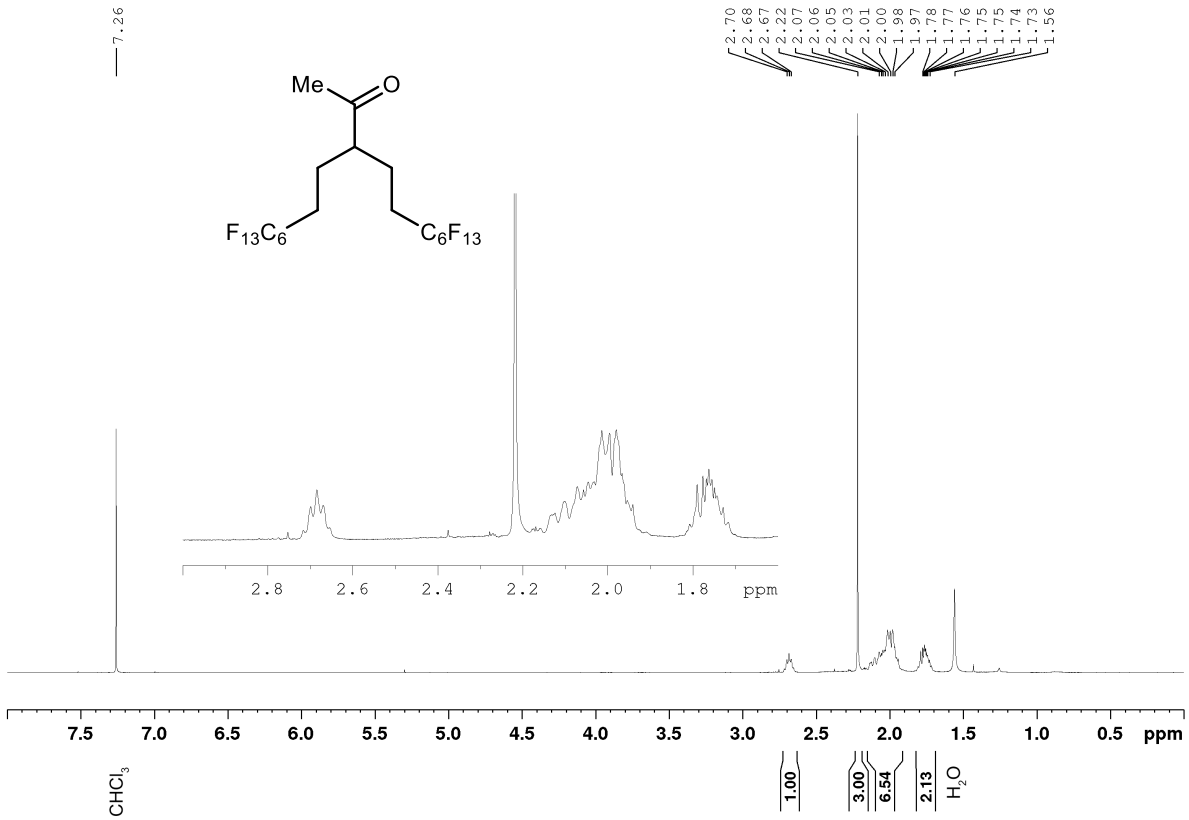

^{1}H NMR (500 MHz, $CDCl_3$) **9**

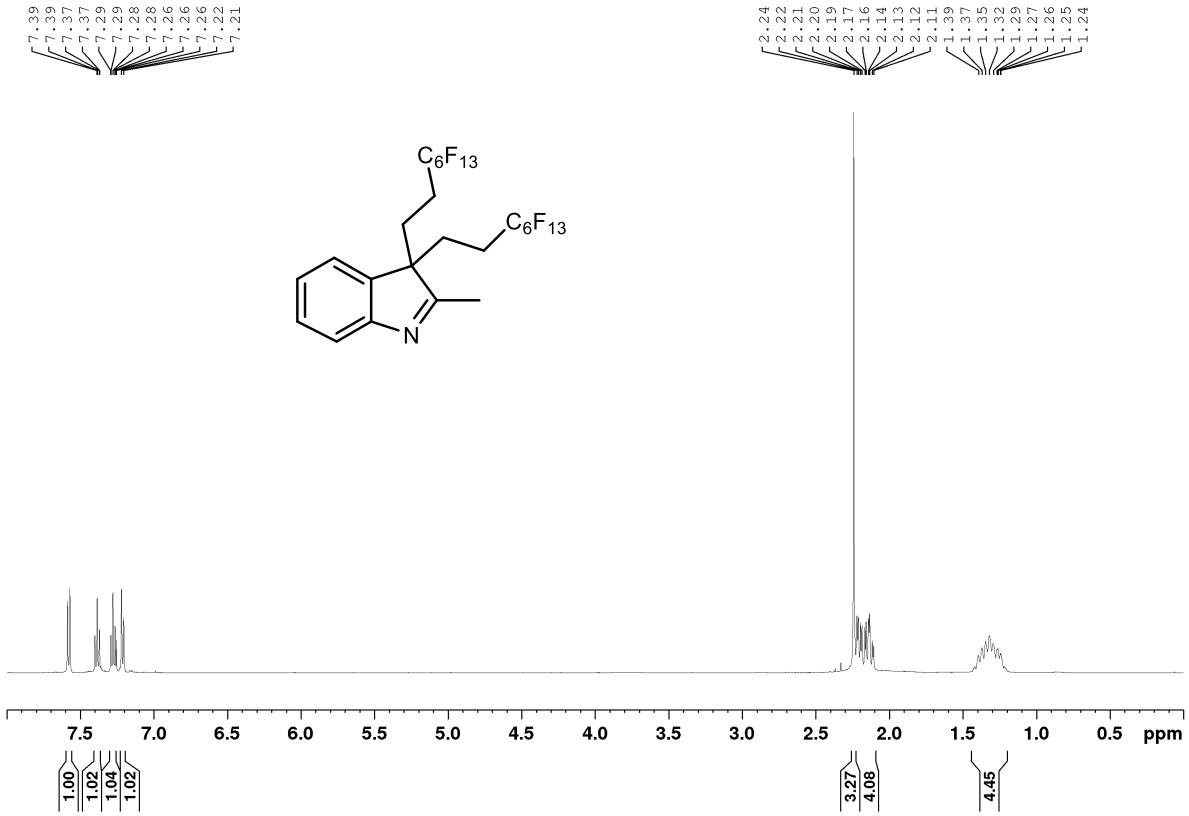

^{1}H NMR (500 MHz, $CDCl_3$) **10**

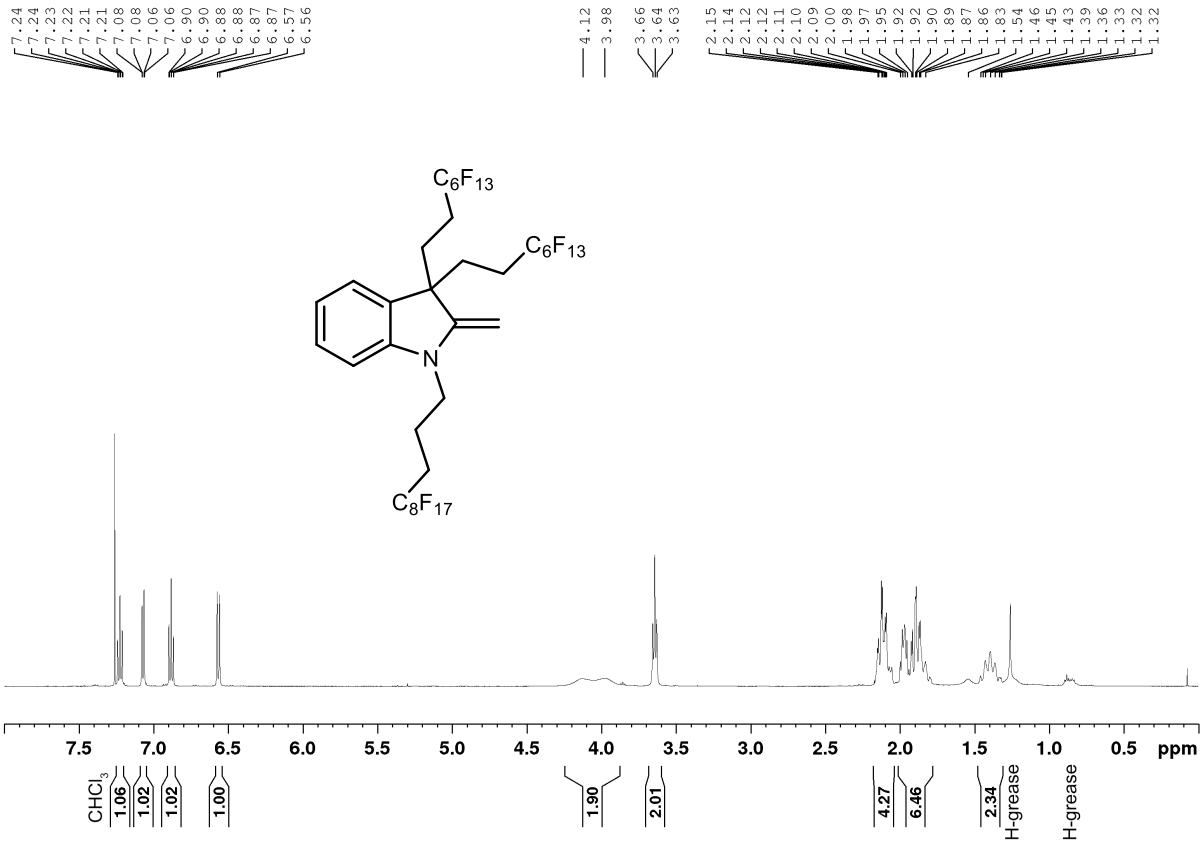

^{1}H NMR (500 MHz, HFIP-d_2) **1a**

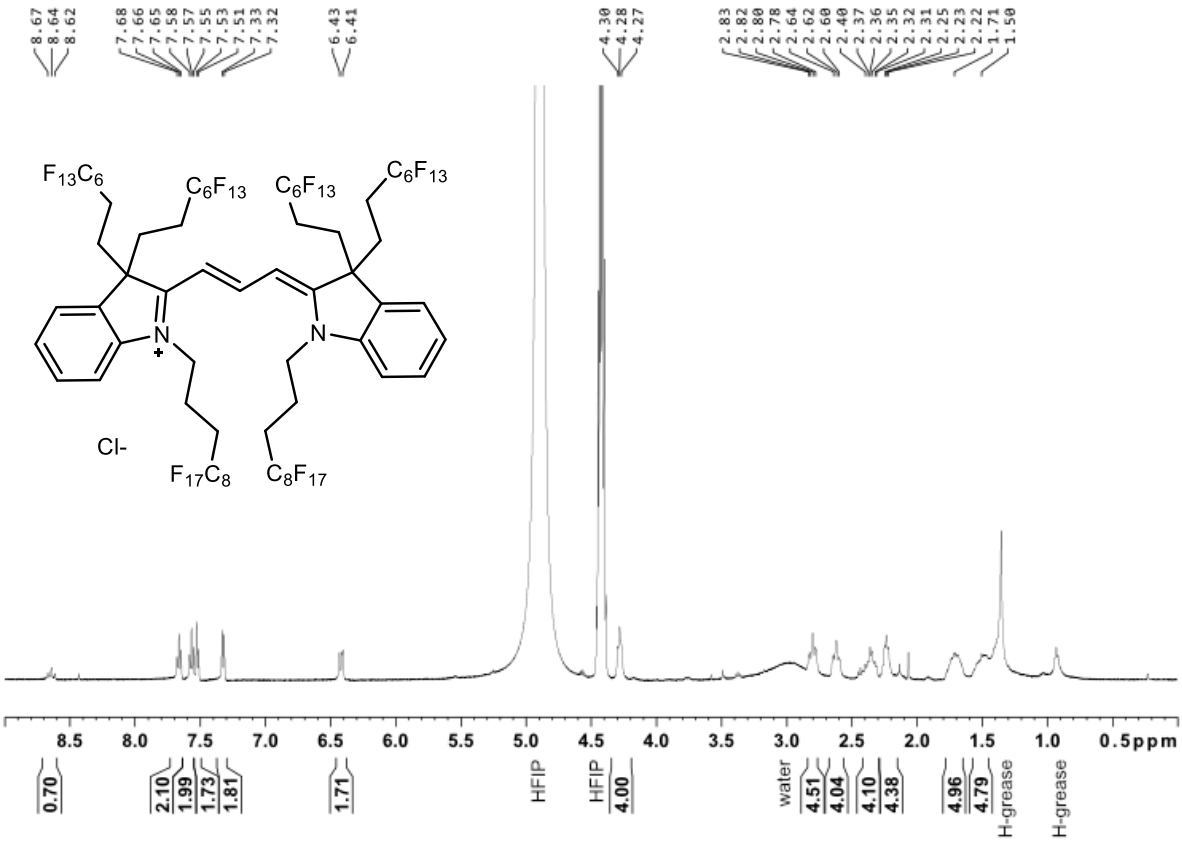

^{1}H NMR (500 MHz, $CDCl_3$) **1b**

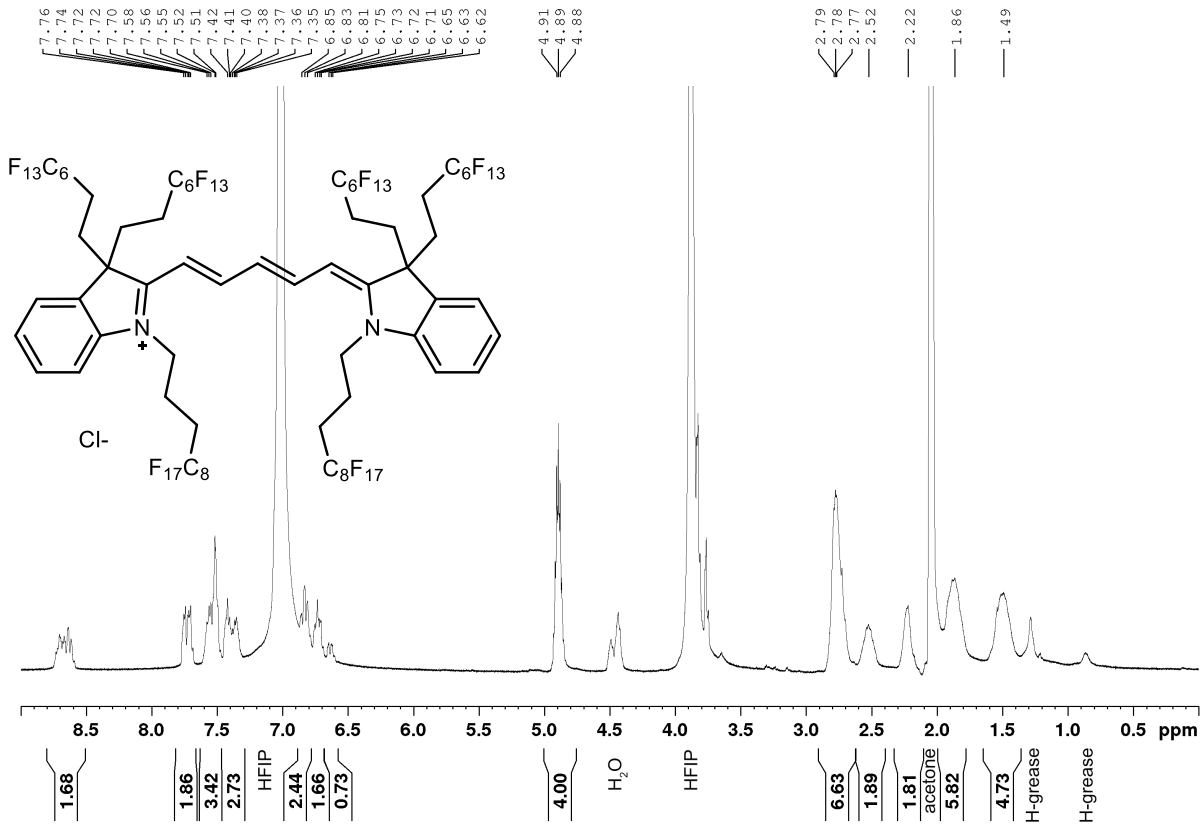

^{1}H NMR (500 MHz, HFIP-d_2) **1c**

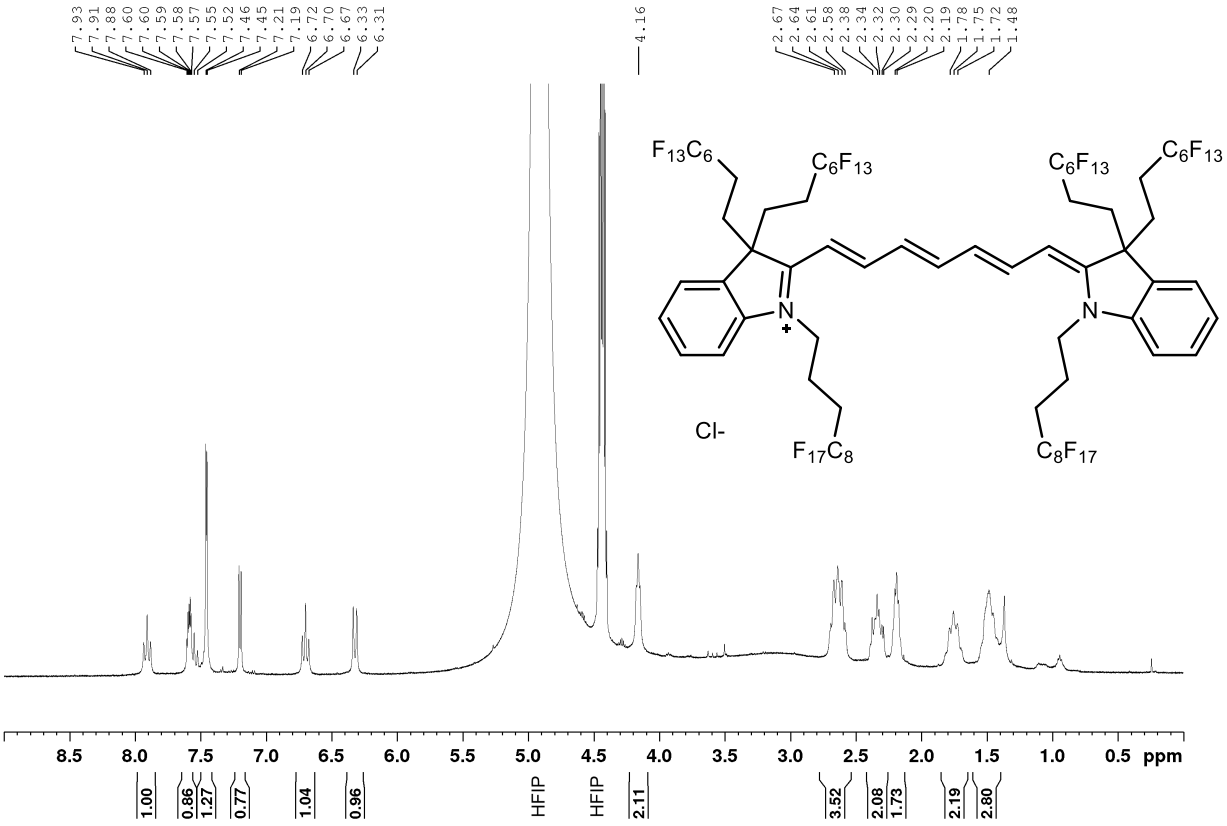

^{13}C NMR (126 MHz, acetone-d_6) **8**

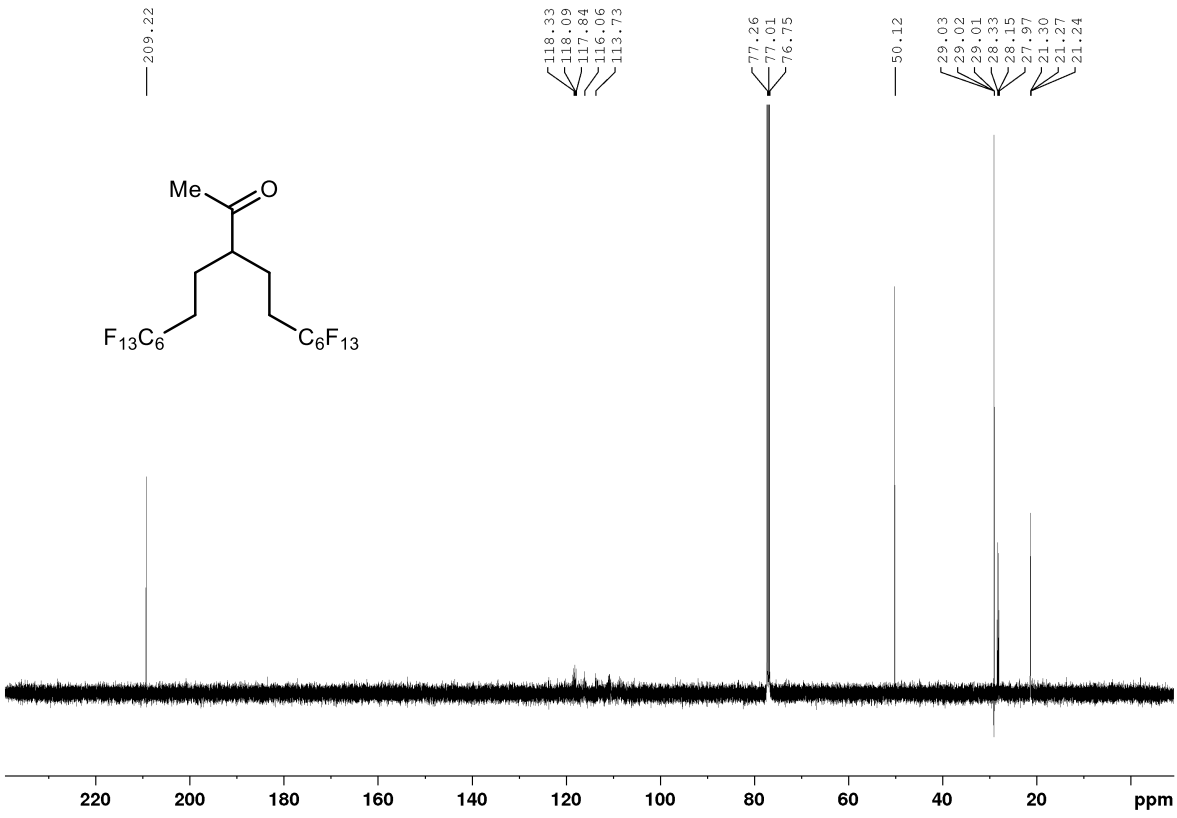

^{13}C NMR (126 MHz, $CDCl_3$) **9**

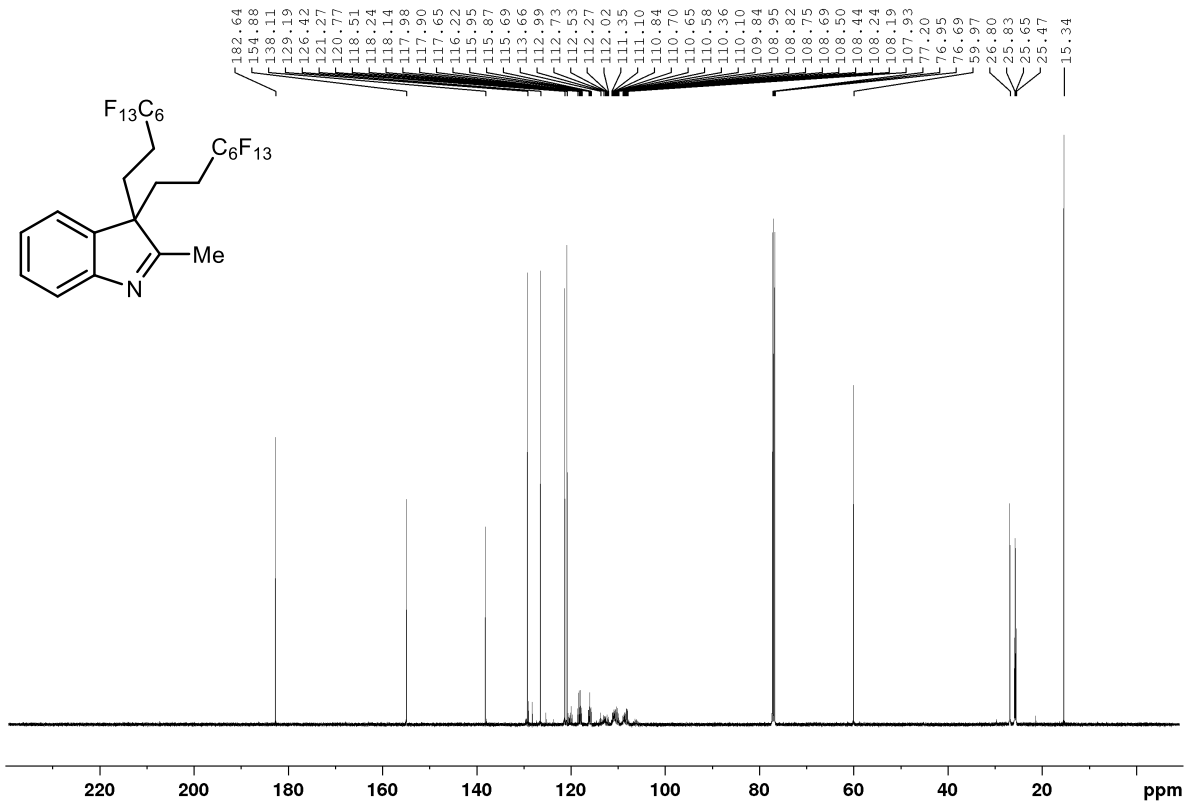

^{13}C NMR (126 MHz, $CDCl_3$) **10**

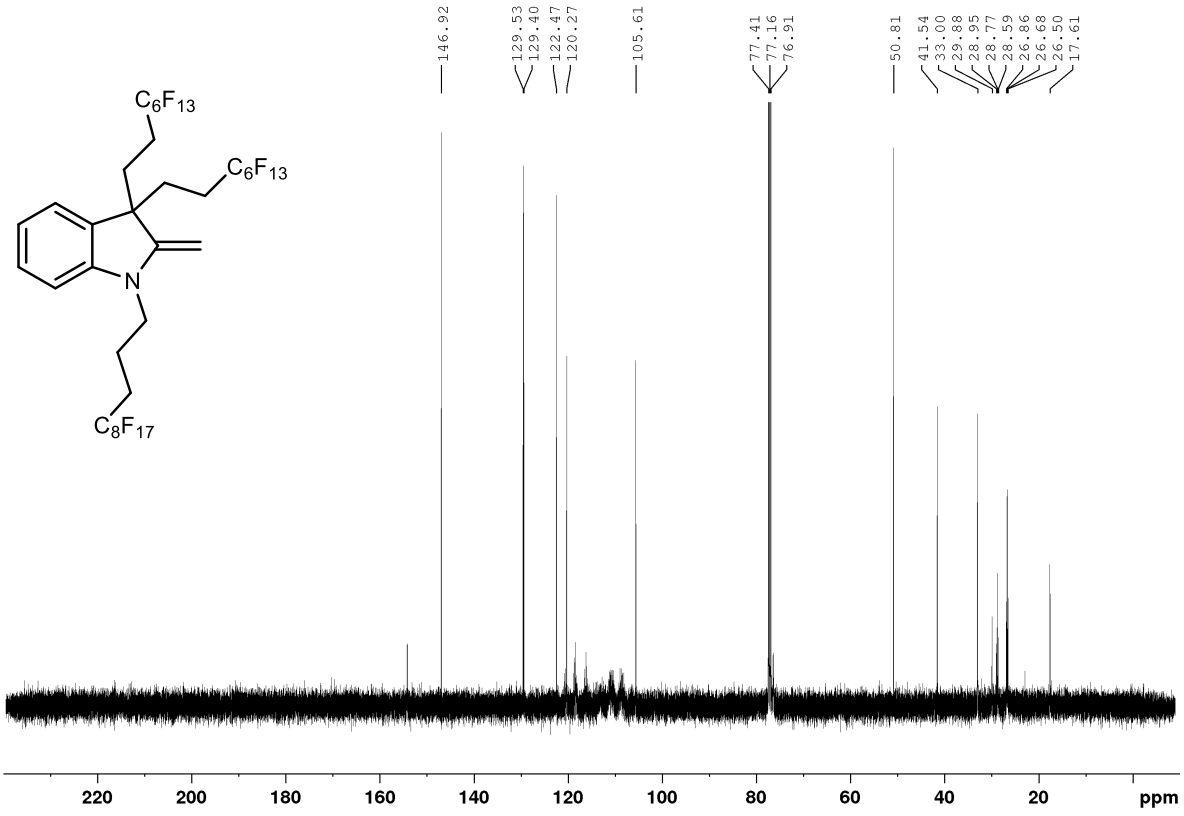

^{19}F NMR (282 MHz, $CDCl_3$) **S1**

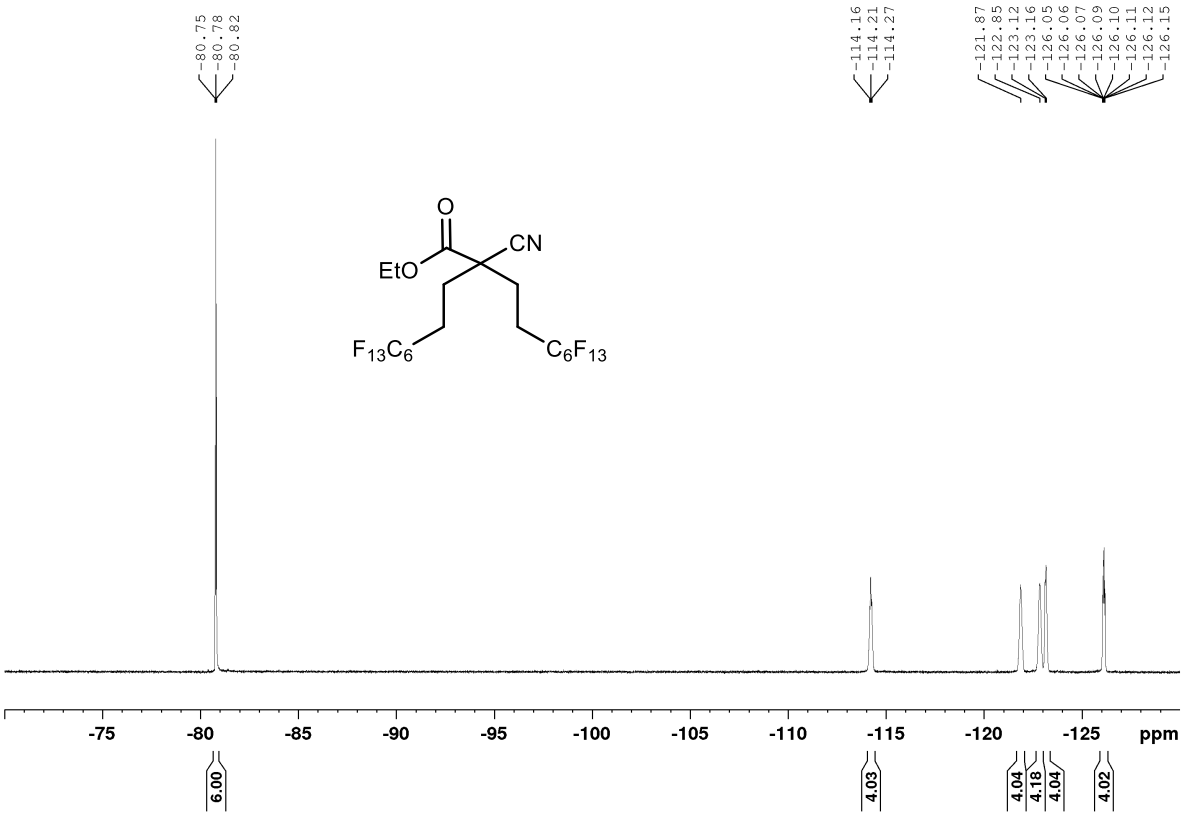

^{19}F NMR (376 MHz, $CDCl_3$) **7**

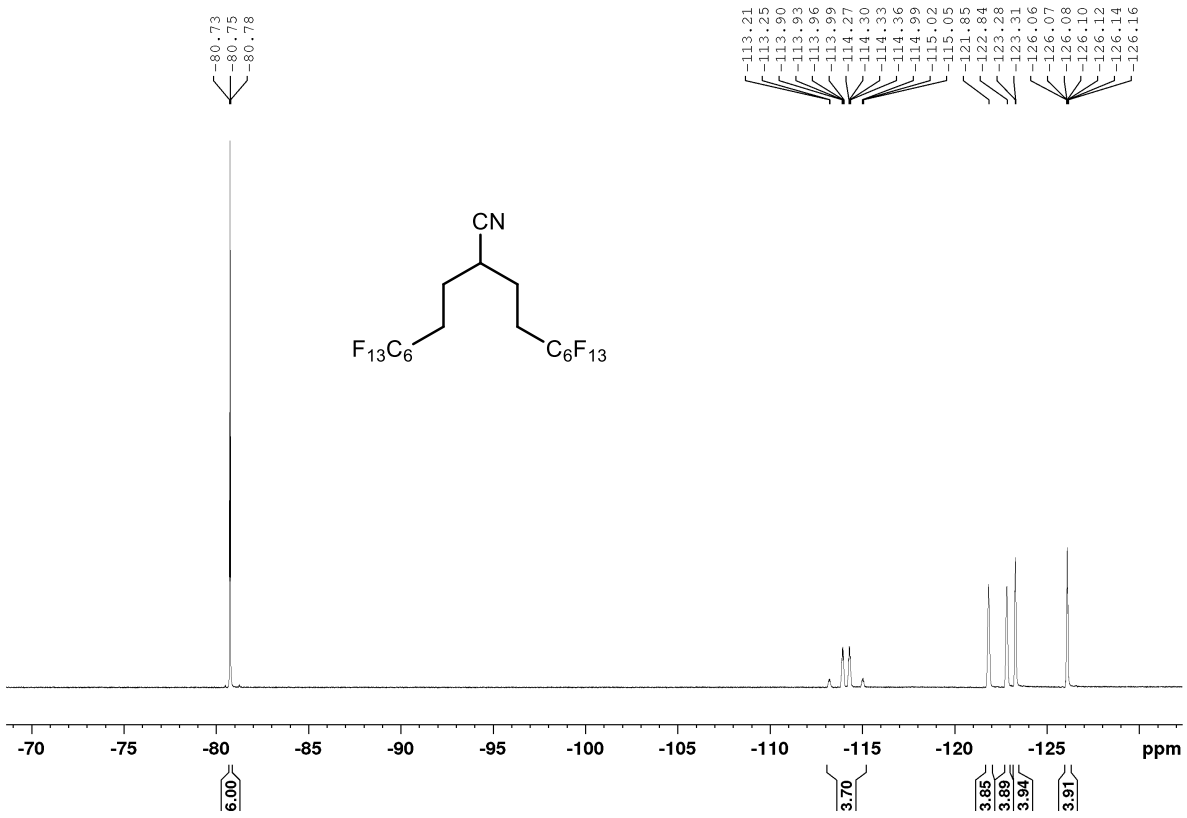

^{19}F NMR (282 MHz, $CDCl_3$) **8**

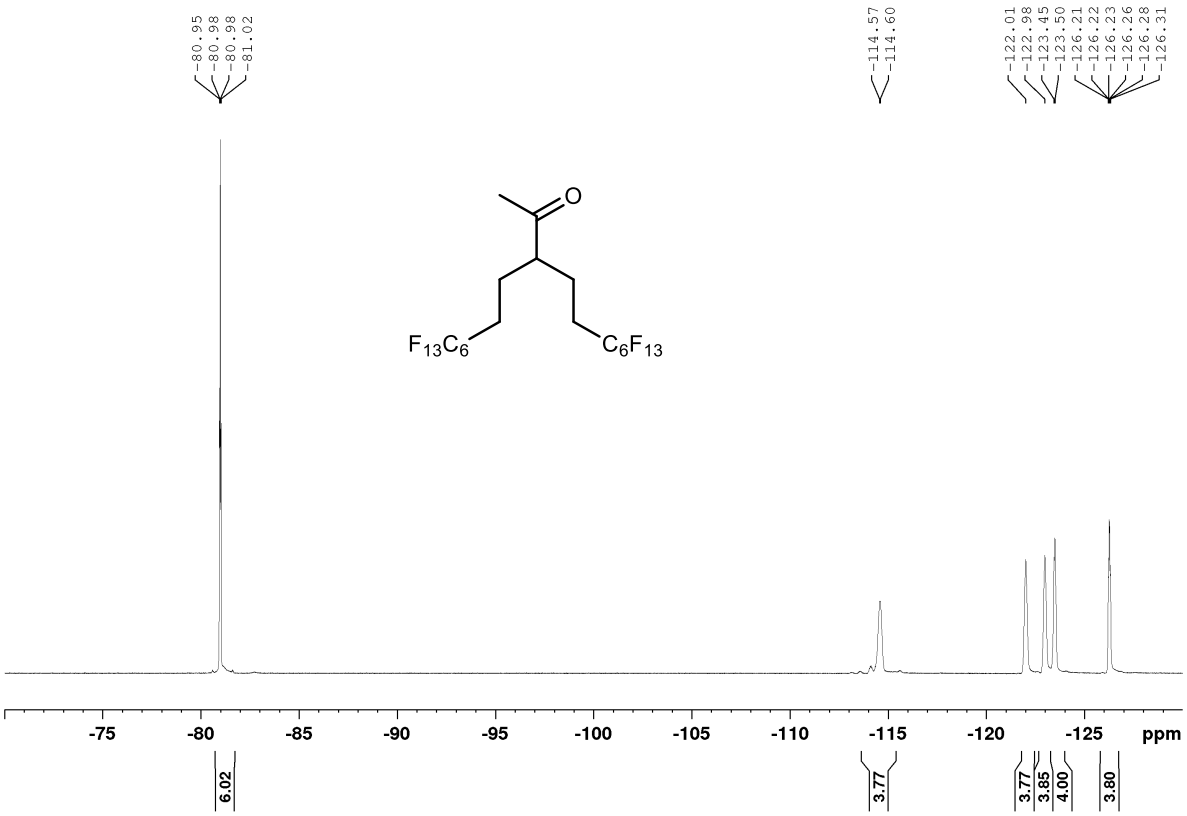

^{19}F NMR (282 MHz, $CDCl_3$) **9**

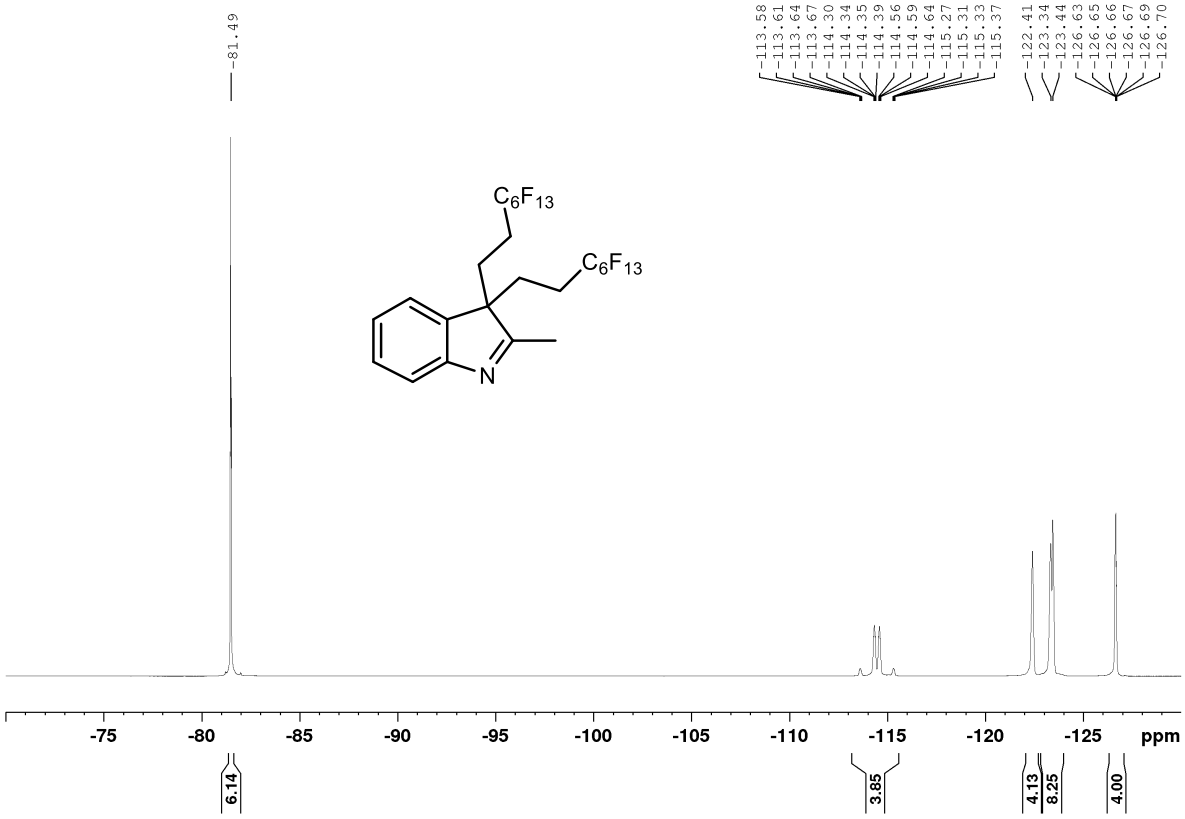

^{19}F NMR (376 MHz, $CDCl_3$) **10**

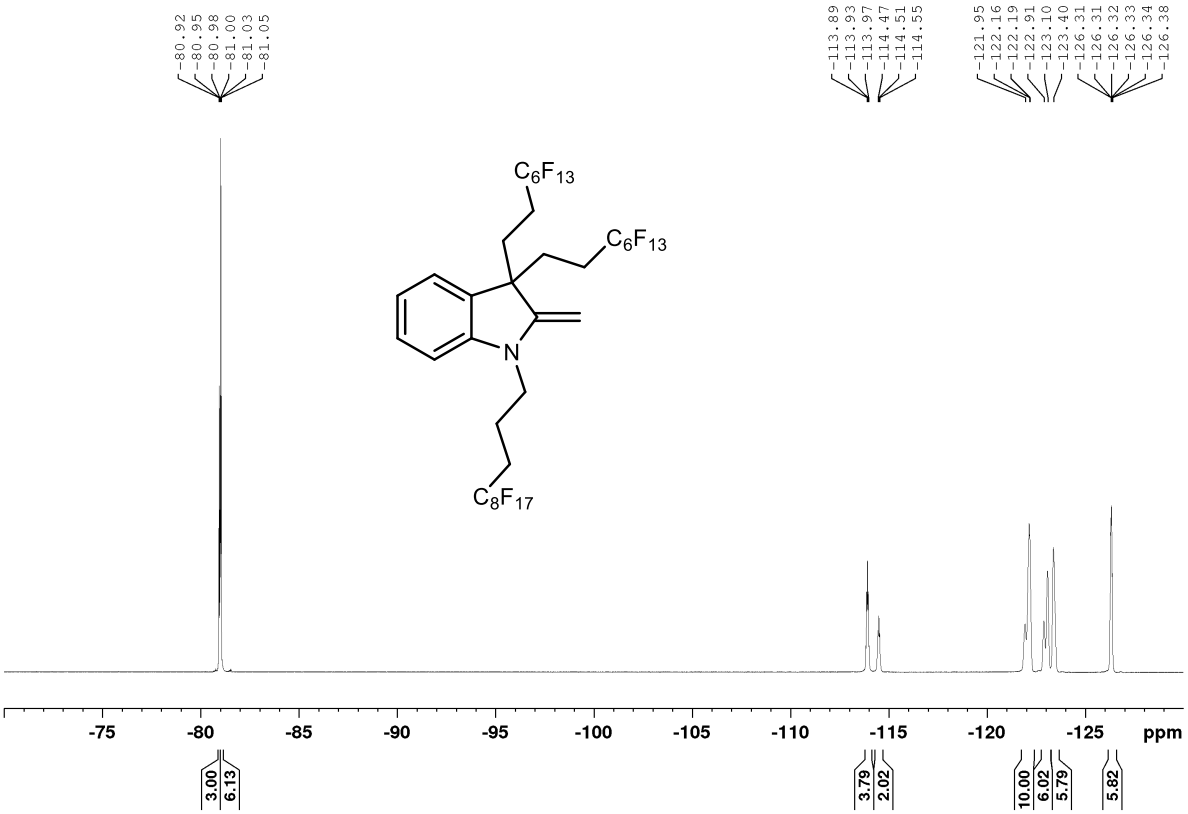

^{19}F NMR (376 MHz, $CDCl_3$) **1a**

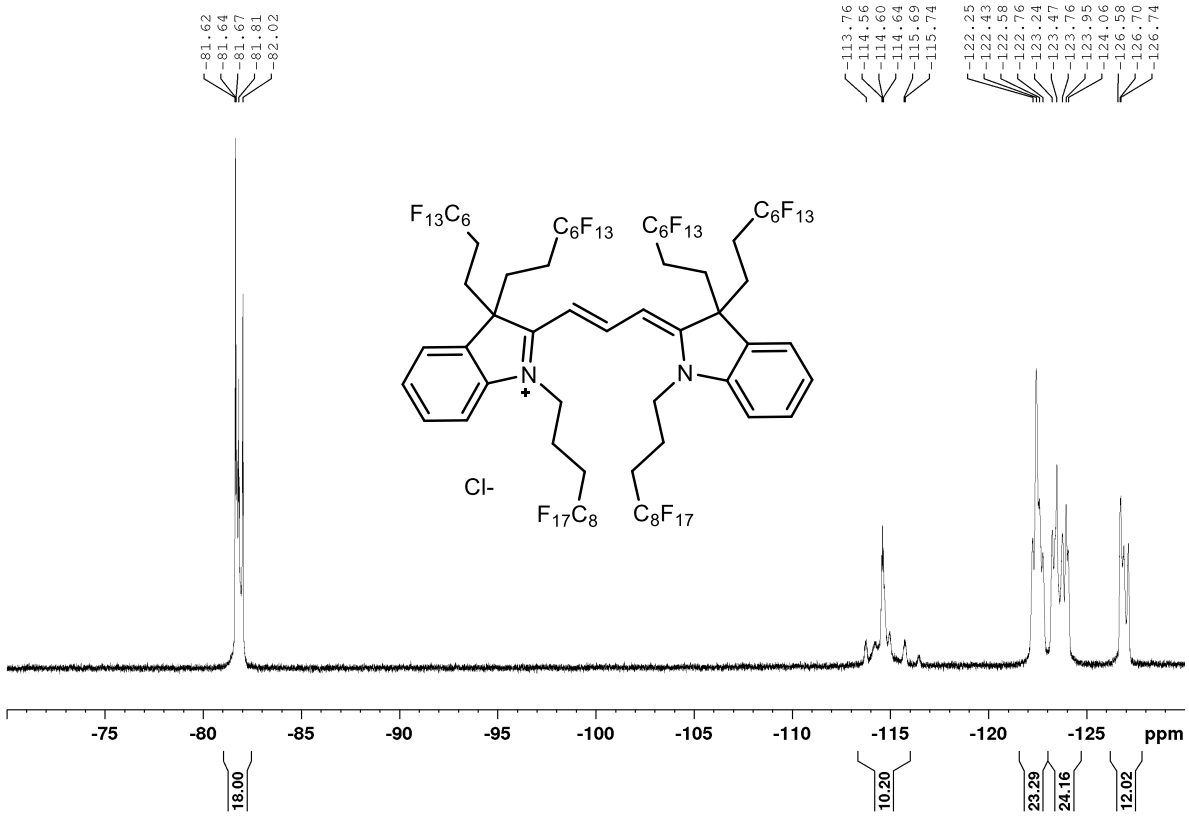

^{19}F NMR (376 MHz, acetone-d_6) **1b**

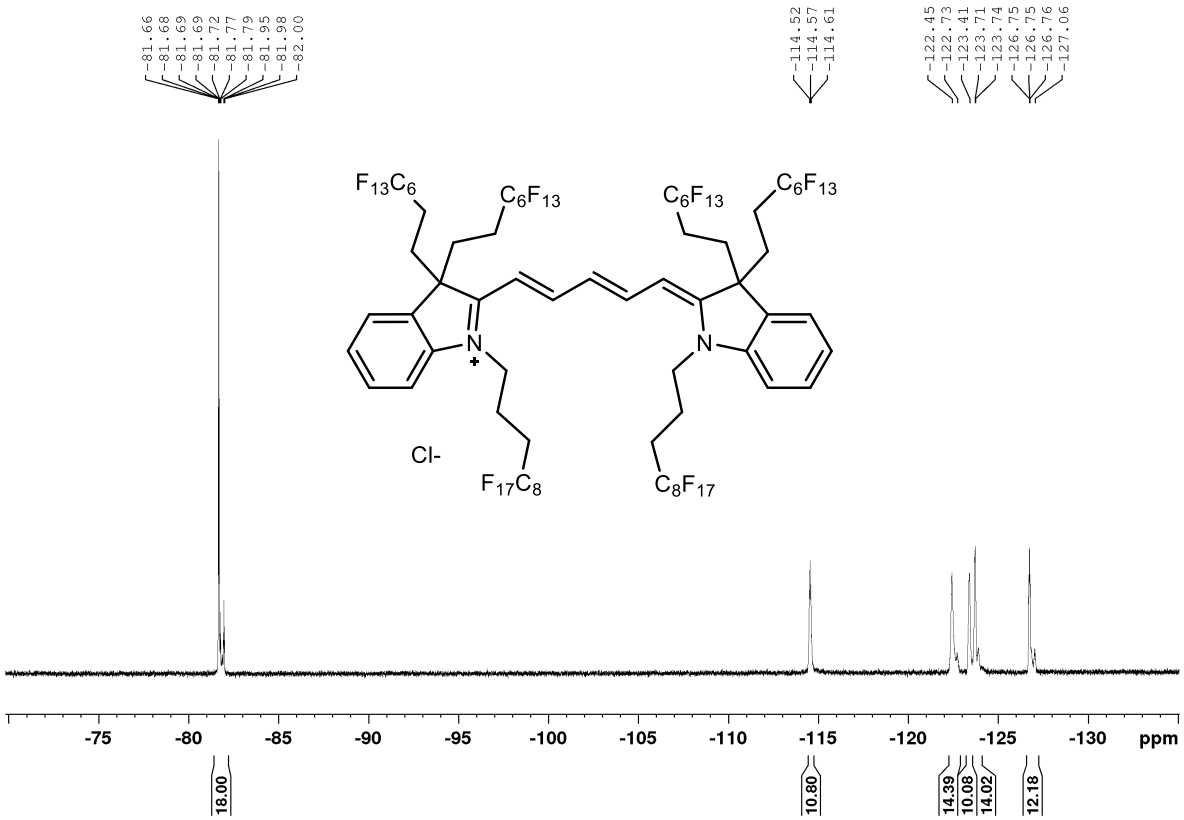

^{19}F NMR (376 MHz, $CDCl_3$) **1c**

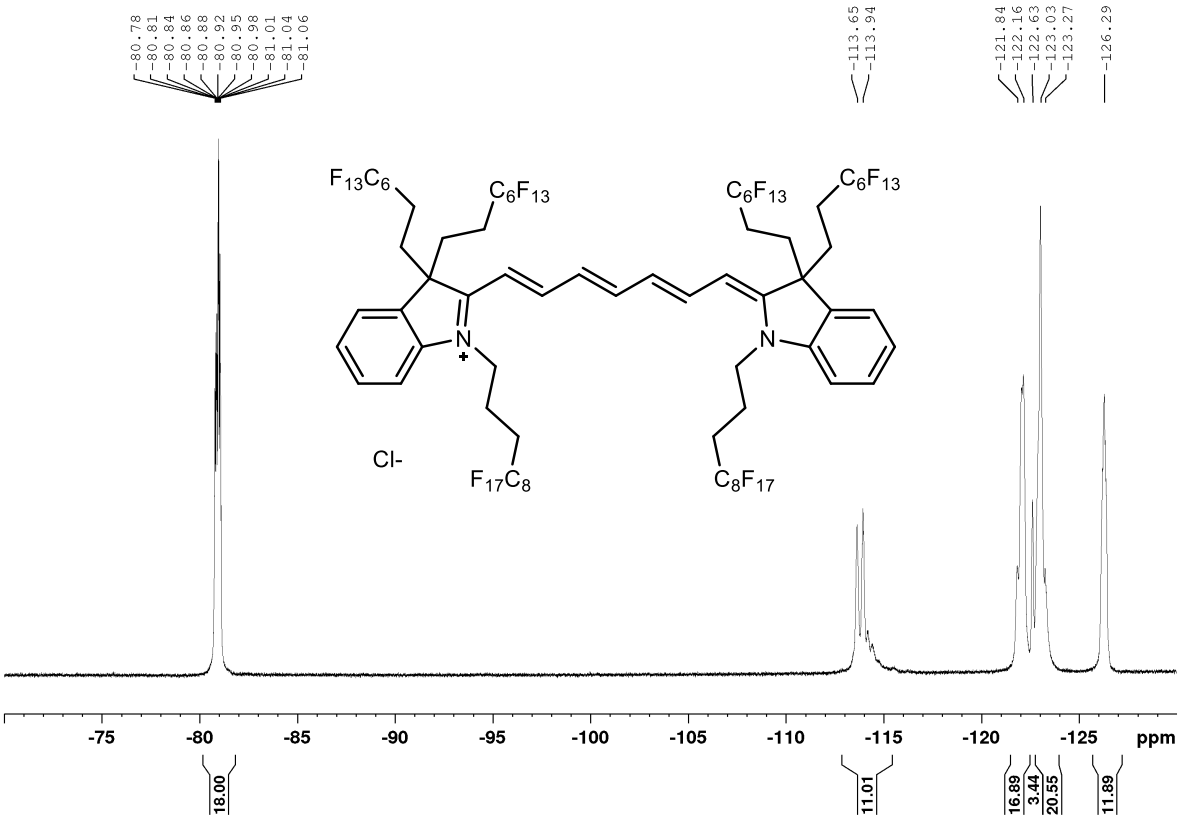

References

(1) Miller, M.A.; Sletten, E.M. A general approach to biocompatible branched fluorous tags for increased solubility in perfluorocarbon solvents. *Org. Lett.* **2018**, *20*, 6850–6854.

(2) Rachael A. Day; Daniel A. Estabrook; Carolyn Wu; John O. Chapman; Alyssa J. Togle; Ellen M. Sletten. Systematic Study of Perfluorocarbon Nanoemulsions Stabilized by Polymer Amphiphiles. ACS Appl. Mater. Interfaces 2020. https://pubs.acs.org/doi/10.1021/acsami.0c07206.

(3) Nusslein-Volhard, R. D. Cellular materials in nature and medicine (Oxford University Press, 2002).

(4) Serwane, F.; Mongera, A.; Rowghanian, P.; Kealhofer, D.A.; Lucio, A.A.; Hockenbery, Z.M.; Campàs, O. In vivo quantification of spatially varying mechanical properties in developing tissues. *Nat. Methods* **2017**, *14*, 181–186.

(5) Mongera, A.; Rowghanian, P.; Gustafson, H.J.; Shelton, E.; Kealhofer, D.A.; Carn, E.K.; Serwane, F.; Lucio, A.A.; Giammona, J.; Campàs, O. A fluid-to-solid jamming transition underlies vertebrate body axis elongation. *Nature* **2018**, *561*, 401–405.

(6) Campas, O. Mammoto, T.; Hasso, S.; Sperling, R.A.; O'Connel, D.; Bixchof, A.G.; Mass, R.; Weitz, D.A. Mahadevan, L.; Ingber, D.E. Quantifying cell-generated mechanical forces within living embryonic tissues. *Nat. Methods* **2014**, *11*, 183–189.

(7) Lucio, A.A.; Mongera, A.; Shelton, E.; Chen, R.; Doyle, A.M.; Campàs, O. Spatiotemporal variation of endogenous cell-generated stresses within 3D multicellular spheroids. *Sci. Rep.* **2017**, 1–11. doi:10.1038/s41598-017-12363-x

(8) Kelm, J.; Timmins N.; Brown C.; Fussenegger M.; Nielsen L. Method for generation of homogeneous multicellular tumor spheroids applicable to a wide variety of cell types. *Biotechnol. Bioeng.* **2003**, *83*, 173–180. doi:10.1002/bit.10655

(9) Shelton, E.; Serwane, F.; Campàs, O. Geometrical characterization of fluorescently labelled surfaces from noisy 3D microscopy data. *J. Microscopy* **2017**, *269*, 259–268.